# Fluorophobic Effect Induces the Self-Assembly of Semifluorinated Tapered Monodendrons Containing Crown Ethers into Supramolecular Columnar Dendrimers Which Exhibit a Homeotropic Hexagonal Columnar Liquid Crystalline Phase

**Virgil Percec,*,† Gary Johansson,† Goran Ungar,‡ and Jianping Zhou‡**

*Contribution from The W. M. Keck Laboratories for Organic Synthesis, Department of Macromolecular Science, Case Western Reserve University, Cleveland, Ohio 44106-7202, and Department of Engineering Materials and Centre for Molecular Materials, University of Sheffield, Sheffield S1 4DU, UK*

*Received May 10, 1996*[⊗]

**Abstract:** The rational design, synthesis, and characterization of the building blocks obtained by the esterification of the first generation of tapered monodendrons 3,4,5-tris(*p*-dodecan-1-yloxy)benzoic acid (**12-AG**) and 3,4,5-tris[*p*-(*n*-dodecan-1-yloxy)benzyloxy]benzoic acid (**12-ABG**) containing semifluorinated dodecyl groups [i.e., **12Fn-AG-15C5** ($n = 0$, 4, 6, 8), **12Fn-AG-B15C5**, **12Fn-ABG-15C5**, and **12Fn-ABG-B15C5** ($n = 0$ and 8) where *n* following the letter F represents the number of outer perfluorinated methylenic units of the dodecyl group] with 4′-hydroxymethyl-(benzo-15-crown-5) (**B15C5**) and 1-hydroxymethyl(15-crown-5) (**15C5**) are described. All building blocks self-assemble into supramolecular cylindrical or rod-like dendrimers *via* ion-mediated complexation processes. These rod-like supermolecules form a thermotropic hexagonal columnar ($\Phi_h$) liquid crystalline (LC) phase. The fluorination of the dodecyl groups of these tapered building blocks enhances dramatically their self-assembly ability. The building blocks based on $n = 6$ and 8 self-assemble into supramolecular columns solely *via* the fluorophobic effect. Direct structural characterization of the supramolecular columns obtained *via* these two molecular recognition processes by a combination of techniques consisting of differential scanning calorimetry, X-ray diffraction, and thermal optical polarized microscopy, and of the columns obtained solely *via* the fluorophobic effect allowed the construction of molecular models for the supramolecular columns obtained *via* these two organizing forces. An increase in the column diameter with increasing *n* and with the complexation of metal salts (i.e., alkali metal trifluoromethanesulfonates) accounts for a structural model in which the uncomplexed and complexed crown ethers are placed side-by-side in the center of the column with the melted tapered side groups radiating toward its periphery. The perfluorinated segments of the building blocks are microsegregated from the perhydrogenated and aromatic segments of the column. The supramolecular columns obtained from building blocks with $n = 8$ align homeotropically in the $\Phi_h$ LC phase on untreated glass slides, i.e., form single crystal liquid crystals in which the long axes of their columns are perpendicular to the glass surface. Both the self-assembly of supramolecular columns induced solely by the fluorophobic effect and the homeotropic alignment of these columns in their $\Phi_h$ LC phase open extremely interesting new synthetic and technologic opportunities in the area of self-assembly of well-defined supramolecular architectures obtained from monodendrons and other building blocks.

## Introduction

One of the most fascinating subjects of research which evolved from the field of dendrimers[1] is concerned with the construction of novel complex molecular, macromolecular, and supramolecular nanoscopic architectures with well defined shapes and functions by using specifically designed monodendrons and dendrimers and/or combinations of dendrimers and other macromolecular topologies as building blocks.[2] The

† Case Western Reserve University. Phone: 216-368-4242. Fax: 216-368-4202. e-mail: vxp5@po.cwru.edu.

‡ University of Sheffield.

⊗ Abstract published in *Advance ACS Abstracts,* October 1, 1996.

(1) For recent reviews and highlights on dendrimers, see: (a) Tomalia, D. A. *Macromol. Symp.* **1996**, *101*, 243. (b) Bell, T. W. *Science* **1996**, *271*, 1077. (c) Bradley, D. *Science* **1995**, 270, 1924. (d) Service, R. F. *Science* **1995**, *267*, 458. (e) Tomalia, D. A. *Sci. Amer.* **1995**, *May*, 62. (f) Newkome, G. R.; Moorefield, C. N. In *Mesomolecules: From Molecules to Materials*; Mendenhall, G. D., Greenberg, A., Liebman, J. F., Eds.; Chapman & Hall: New York, 1995; p 27. (g) Ardoin, N.; Astruc, D. *Bull. Soc. Chim. Fr.* **1995**, 875. (h) Young, J. K.; Moore, J. S. In *Modern Acetylene Chemistry*; Stang, P. J., Diederich, F., Eds.; VCH: Weinheim, 1995; p 415. (i) Fréchet, J. M. J. *Science* **1994**, *263*, 1710. (j) Vögtle, F.; Issberner, J.; Moors, R. *Angew. Chem., Int. Ed. Engl.* **1994**, *33*, 2413. (k) *Advances in Dendritic Macromolecules*; Newkome, G. R., Ed.; JAI Press, Inc.: Greenwich, 1994; Vol. 1. (l) Tomalia, D. A. *Adv. Mater.* **1994**, *6*, 529. (m) Escamilla, G. H.; Newkome, G. R. *Angew. Chem., Int. Ed. Engl.* **1994**, *33*, 1937. (n) Tomalia, D. A.; Durst, H. D. *Top. Curr. Chem.* **1993**, *165*, 193. (o) Dvornic, P. R.; Tomalia, D. A. *Chem. Brit.* **1994**, 641.

(2) For a few recent examples on the design of new complex architectures and shapes from dendrimers, see: (dendrimer box) (a) Jansen, J. F. G. A.; de Brabander-van den Berg, E. M. M.; Meijer, E. W. *Science* **1994**, *266*, 1226. (b) Jansen, J. F. G. A.; Janssen, R. A. J.; de Brabander-van den Berg, E. M. M.; Meijer, E. W. *Adv. Mater.* **1995**, *7*, 561. (c) Jansen, J. F. G. A.; Meijer, E. W.; de Brabander-van den Berg, E. M. M. *J. Am. Chem. Soc.* **1995**, *117*, 4417. (molecular ball bearings) (d) Hawker, C. J.; Farrington, P. J.; MacKay, M. E.; Wooley, K. L.; Fréchet, J. M. J. *J. Am. Chem. Soc.* **1995**, *117*, 4409. (sugar balls) (e) Aoi, K.; Itoh, K.; Okada, M. *Macromolecules* **1995**, *28*, 5391. (chiral dendritic surfaces) (f) Jansen, J. F. G. A.; Peerlings, H. W. I.; de Brabander-van den Berg, E. M. M.; Meijer, E. W. *Angew. Chem., Int. Ed. Engl.* **1995**, *34*, 1206 and references cited therein. (well-defined micellar aggregates from dendrimers containing block copolymers and amphiphilic surfaces) (g) Hawker, C. J.; Fréchet, J. M. J. *J. Am. Chem. Soc.* **1992**, *114*, 8405. (h) Newkome, G. R.; Moorefield, C. N.; Keith, J. M.; Baker, G. R.; Escamilla, G. H. *Angew. Chem., Int. Ed. Engl.* **1994**, *33*, 666. (i) Fréchet, J. M. J.; Gitsov, I. *Macromol. Symp.* **1995**, *98*, 441. (j) Gitsov, I.; Fréchet, J. M. J. *J. Am. Chem. Soc.* **1996**, *118*, 3785. (k) van Hest, J. C. M.; Delnoye, D. A. P.; Baars, M. W. P. L.; van Genderen, M. H. P.; Meijer, E. W. *Science* **1995**, *268*, 1592. (l) Chapman, T. M.; Hillyer, G. L.; Mahan, E. J.; Shaffer, K. A. *J. Am. Chem. Soc.* **1994**, *116*, 11195. (m) Hawker, C. J.; Wooley, K. L.; Fréchet, J. M. J. *J. Chem. Soc., Perkin Trans. 1* **1993**, 1287.

S0002-7863(96)01573-9 CCC: $12.00 

synthetic capabilities of this field increased dramatically after the convergent approach to dendrimers was developed.[3] Nevertheless, the expansion of this field relies on the availability of accelerated synthetic methods for the preparation of both monodendrons and dendrimers.[4] Consequently, the use of supramolecular chemistry to self-assemble monodendrons into supramolecular dendrimers may generate synthetic strategies[5] which are at least complementary to those based on covalent chemistry. The molecular recognition process which was the most exploited both in the construction of monodendrons and of dendrimers is based on various metal binding strategies.[6] Although molecular recognition strategies based on hydrogen bonding were employed in the self-assembly of various macromolecular systems,[7a] it was only very recently that they were applied to the functionalization[7b] and self-assembly of dendrimers[7c] in solution. A particular self-assembly event can be dominated by a single molecular recognition process based on either hydrogen bonding, van der Waals interactions, electrostatic interactions, and the hydrophobic effect.[8] However, all these processes are cooperative, and their contribution could be equally important not only in the aggregation process but also especially in the stabilization of a unique architecture. While most molecular recognition processes are based on attractive exoenthalpic forces, the hydrophobic effect provides a unique organizing force based on repulsion by the solvent or by other dissimilar parts of the same molecule.[8]

Little is presently known about the design of dendrimers which exhibit a well-defined shape in solution, in melt phase, or solid state, and even less is understood about the change of their shape at the transition from solution to melt and to solid state.[1e,i,n] For example, in solution a transition from an extended to a globular shape was theoretically predicted[1in,9] and experimentally supported by a plot of intrinsic viscosity *versus* molecular weight[10] and by other indirect methods.[1i] However, in solid state the same dendrimers are amorphous.[1i,2d,11] A cylindrical shape was suggested without any experimental evidence for a poly(*p*-phenylene) containing Fréchet type monodendrons as side groups.[12] Rod-like dendrimers were reported by Tomalia[13] by attaching poly(amidoamine) monodendrons to a linear polyethyleneimine, and supramolecular disc-like hexameric dendrimers were recently self-assembled *via* an elegant exact H-bonding.[1b,7c] All this indirect experimental evidence for spherical[6f,14a−c] and rod-like[14d] shapes obtained from dendrimers is strongly supported by their direct visualization *via* transmission electron and atomic force microscopy which, however, cannot easily discriminate between individual and aggregated dendrimers.

Direct determination of the shape and of the internal structure of the dendrimer within this shape can be obtained only from X-ray diffraction experiments. Several years ago we initiated a research program to design monodendrons which produce macromolecular and supramolecular dendrimers that generate well-defined shapes in solid and melt states. Two different synthetic approaches are investigated toward this goal. One is based on the use of $AB_2$ rod-like conformationally flexible building blocks which produce monodendrons and macromolecular dendrimers which display thermotropic calamitic nematic and smectic liquid crystalline (LC) phases in addition to a crystalline phase.[15] Characterization of LC and crystalline phases of these monodendrons and dendrimers by a combination of various techniques including X-ray diffraction demonstrated, as expected, an elongated rather than a globular shape. The other approach is based on the design of various generations of monodendrons which exhibit a tapered shape.[16−19] These tapered monodendrons are functionalized with suitable *endo*-receptors such as crown ethers, polypodands or with a polymerizable group. Ion-mediated electrostatic and H-bonding recognition processes[16] and/or polymerization reactions[17] self-assemble these building blocks in solution, melt phase and in solid state into a cylindrical or rod-like supramolecular architecture which is responsible for the formation of a thermotropic hexagonal columnar ($\Phi_h$) LC phase. This LC phase warrants a thermodynamically controlled self-assembly process and its characterization by X-ray diffraction provides direct information on the shape and size of the cylindrical supramolecular dendrimer as well as on the arrangement of the monodendrons within the column.[16−19]

(3) For the convergent synthetic approach to dendrimers, see: (a) Hawker, C. J.; Fréchet, J. M. J. *J. Chem. Soc., Chem. Commun.* **1990**, 1010. (b) Hawker, C. J.; Fréchet, J. M. J. *J. Am. Chem. Soc.* **1990**, *112*, 7638. (c) Miller, T. M.; Neenan, T. X. *Chem. Mater.* **1990**, *2*, 346.

(4) For new accelerated synthetic methods to monodendrons and dendrimers, see: (a) Spindler, R.; Fréchet, J. M. J. *J. Chem. Soc., Perkin Trans. 1* **1993**, 913. (b) Wooley, K. L.; Hawker, C. J.; Fréchet, J. M. J. *J. Am. Chem. Soc.* **1991**, *113*, 4252. (c) Twyman, L. J.; Beezer, A. E.; Mitchell, J. C. *J. Chem. Soc., Perkin Trans. 1* **1994**, 407. (d) Fréchet, J. M. J.; Henmi, M.; Gitsov, I.; Aoshima, S.; Leduc, M. R.; Grubbs, R. B. *Science* **1995**, *269*, 1080. (e) Hawker, C. J.; Fréchet, J. M. J.; Grubbs, R. B.; Dao, J. *J. Am. Chem. Soc.* **1995**, *117*, 10763.

(5) Lehn, J. M. *Supramolecular Chemistry*; VCH: Weinheim, 1995.

(6) For selected examples of recent publications on various metal-binding strategies used in the construction of dendrimers, see: (a) Serroni, S.; Denti, G.; Campagna, S.; Ciano, M.; Balzani, V. *J. Am. Chem. Soc.* **1992**, *114*, 2944. (b) Constable, E. C.; Harverson, P. *Chem. Commun.* **1996**, 33. (c) Newkome, G. R.; Güther, R.; Cardullo, F. *Macromol. Symp.* **1995**, *98*, 467. (d) Campagna, S.; Giannetto, A.; Serroni, S.; Denti, G.; Trusso, S.; Mallamace, F.; Micali, N. *J. Am. Chem. Soc.* **1995**, *117*, 1754. (e) Liao, Y.-H.; Moss, J. R. *Organometallics* **1995**, *14*, 2130. (f) Huck, W. T. S.; van Veggel, F. C. J. M.; Kropman, B. L.; Blank, D. M. A.; Keim, E. G.; Smithers, M. M. A.; Reinhoudt, D. N. *J. Am. Chem. Soc.* **1995**, *117*, 8293 and references cited therein.

(7) (a) Lehn, J.-M. *Makromol. Chem., Macromol. Symp.* **1993**, *69*,1. (b) Newkome, G. R.; Moorefield, C. N.; Güther, R.; Baker, G. R. *Am. Chem. Soc. Div. Polym. Chem., Polym. Prepr.* **1995**, *36(1)*, 609. (c) Zimmerman, S. C.; Zeng, F.; Reichert, D. E. C.; Kolotuchin, S. V. *Science* **1996**, *271*, 1095.

(8) (a) Schneider, H.-J. *Angew. Chem., Int. Ed. Engl.* **1991**, *30*, 1417. (b) Tanford, C. *Science* **1978**, *200*, 1012. (c) Buckingham, A. D. In *Principles of Molecular Recognition*; Buckingham, A. D., Legon, A. C., Roberts, S. M., Eds.; Chapman & Hall: London, 1993; p 1. (d) Ciferri, A. *Progr. Polym. Sci.* **1995**, *20*, 1081.

(9) (a) de Gennes, P. G.; Hervet, H. *J. Phys. Lett. (Paris)* **1983**, *44*, 35. (b) Naylor, A. M.; Goddard, III, W. A.; Keifer, G.; Tomalia, D. A. *J. Am. Chem. Soc.* **1989**, *111*, 2339. (c) Lescanec, R. L.; Muthukumar, M. *Macromolecules* **1990**, *23*, 2280.

(10) Mourey, T. H.; Turner, S. R.; Rubinstein, M.; Fréchet, J. M. J.; Hawker, C. J.; Wooley, K. L. *Macromolecules* **1992**, *25*, 2401.

(11) Wooley, K. L.; Hawker, C. J.; Pochan, J. M.; Fréchet, J. M. J. *Macromolecules* **1993**, *26*, 154.

(12) (a) Frendenberger, R.; Claussen, W.; Schlueter, A.-D.; Wallmeier, H. *Polymer* **1994**, *35*, 4496. (b) Claussen, W.; Schulte, N.; Schlueter, A.-D. *Macromol. Rapid Commun.* **1995**, *16*, 89. (c) Schlueter, A.-D.; Claussen, W.; Frendenberger, R. *Macromol. Symp.* **1995**, *98*, 475.

(13) See: Tomalia, D. A. in ref 1n, p 229 and private communication.

(14) (a) Tomalia, D. A.; Baker, H.; Dewald, J.; Hall, M.; Kallos, G.; Martin, S.; Roeck, J.; Ryder, J.; Smith, P. *Polym. J. (Japan)* **1985**, *17*, 117. (b) Tomalia, D. A.; Baker, H.; Dewald, J.; Hall, M.; Kallos, G.; Martin, S.; Ryder, J.; Smith, P. *Macromolecules* **1986**, *19*, 2466. (c) Newkome, G. R.; Yao, Z.; Baker, G. R.; Gupta, V. K.; Russo, P. S.; Saunders, M. J. *J. Am. Chem. Soc.* **1986**, *108*, 849. (d) Newkome, G. R.; Moorefield, C. N.; Baker, G. R.; Behera, R. K.; Escamilla, G. H.; Saunders, M. J. *Angew. Chem., Int. Ed. Engl.* **1992**, *31*, 917.

(15) Percec, V.; Chu, P.; Ungar, G.; Zhou, J. *J. Am. Chem. Soc.* **1995**, *117*, 11441.

(16) For experiments which concluded that tapered monodendrons containing crown ethers and polypodands self-assemble *via* ion-mediated and H-bonding processes into supramolecular rod-like shapes, see: (a) Percec, V.; Heck, J. *Am. Chem. Soc. Div. Polym. Chem., Polym. Prepr.* **1992**, *33(1)*, 217. (b) Percec, V.; Johansson, G.; Heck, J.; Ungar, G.; Batty, S. V. *J. Chem. Soc., Perkin Trans. 1* **1993**, 1411. (c) Percec, V.; Heck, J.; Tomazos, D.; Falkenberg, F.; Blackwell, H.; Ungar, G. *J. Chem. Soc., Perkin Trans. 1* **1993**, 2799. (d) Percec, V.; Heck, J. A.; Tomazos, D.; Ungar, G. *J. Chem. Soc., Perkin Trans. 2* **1993**, 2381. (e) Johansson, G.; Percec, V.; Ungar, G.; Abramic, D. *J. Chem. Soc., Perkin Trans. 1* **1994**, 447. (f) Percec, V.; Tomazos, D.; Heck, J.; Blackwell, H.; Ungar, G. *J. Chem. Soc., Perkin Trans. 2* **1994**, 31. (g) Tomazos, D.; Out, G.; Heck, J. A.; Johansson, G.; Percec, V.; Möller, M. *Liq. Cryst.* **1994**, *16*, 509. (h) Ungar, G.; Batty, S. V.; Percec, V.; Heck, J.; Johansson, G. *Adv. Mat. Opt. Electr.* **1994**, *4*, 303.

It is well established that perfluorinated alkanes are more rigid and linear and due to their extremely low surface energy less miscible than the corresponding perhydrogenated alkanes (fluorophobic effect).[20] Consequently, the replacement of a perhydrogenated alkane with a perfluorinated one in the tail of a rigid rod-like molecular LC enhances the thermal stability of calamitic LC phases.[21] At the same time, the combination of a suitable length and ratio of perfluorinated and perhydrogenated alkane segments within the same molecule produces a microsegregation at the molecular level, and this process has been shown to be alone responsible for the formation of highly ordered lamellar thermotropic[22,23] and lyotropic mesophases.[24] Recently, we discovered a dramatic *stabilization* of the $\Phi_h$ LC phase generated from supramolecular and macromolecular columns *via* semifluorination of the alkyl groups of their tapered building blocks.[25] A dramatic *enhancement* of the ability of semifluorinated tapered building blocks to self-assemble into supramolecular columns which produce $\Phi_h$ phases via H-bonding processes was also demonstrated.[26] Finally, the *stabilization* of the $\Phi_h$ phase generated from fluoroalkylated discotic molecules was reported by Ringsdorf *et al*.[27] This extremely broad range of capabilities of the fluorophobic effect, which represents an amplification of the hydrophobic effect, to stabilize LC phases prompted us to investigate its potential in the design of tapered monodendrons which self-assemble solely *via* the fluorophobic effect.

The goal of this paper is to report the rational design, synthesis, and characterization of the simplest tapered monodendrons containing crown ethers which self-assemble into cylindrical or rod-like supramolecular dendrimers which display a thermotropic $\Phi_h$ LC phase solely *via* the fluorophobic effect. The structure of these supramolecular rod-like dendrimers determined by X-ray diffraction experiments was compared with that of the corresponding assemblies generated *via* a combination of fluorophobic and ion-mediated interactions. These experiments provide the first structural comparison of the two supramolecular systems assembled either by ion-mediated processes or by the fluorophobic effect and demonstrate the extraordinary potential of the fluorophobic effect in supramolecular chemistry.

## Results and Discussion

**Rationale, Molecular Design, and Synthesis.** Scheme 1 outlines the self-assembly of the building blocks obtained by the esterification of first generation 3,4,5-tris(*p*-dodecyloxybenzyloxy)benzoic acid (**12-ABG**) and 3,4,5-tris(*p*-dodecyloxy)benzoic acid (**12-AG**) monodendrons with 4′-hydroxymethyl(benzo-15-crown-5) (**B15C5**) and 1-hydroxymethyl(15-crown-5) (**15C5**) (i.e., **12-ABG-B15C5**, **12-ABG-15C5**, **12-AG-B15C5**, **12-AG-15C5**) mediated by the complexation of their crown ether with Li, Na, and K trifluoromethanesulfonates (MOTf).[16b,e,19a,e,f] The tapered group of these building blocks (brick) is responsible for the cylindrical or rod-like shape of the self-assembled architecture. Simultaneously, the crown ether overcomes *via* its interaction with MOTf (mortar) the entropy loss during the self-assembly process and determines the stability of the resulted supramolecular column. These columns are stable in solution, melt phase, and solid state. X-ray investigations performed in the $\Phi_h$ phase indicated a column structure in which the crown ethers are placed side-by-side in the center of the column with their tapered side groups radiating toward its periphery. In the absence of ion complexation these building blocks form lamellar crystals. Since the formation of liquid crystalline phases are thermodynamically controlled processes,[28] this guarantees a thermodynamically controlled self-assembly

(17) For experiments which demonstrate that polymers containing tapered monodendrons which conceptually were derived from hemiphasmidic mesogens produce macromolecular rod-like architectures, see: (a) Percec, V.; Heck, J. *Am. Chem. Soc. Div. Polym. Chem., Polym. Prepr.* **1989**, *30-(2)*, 450. (b) Heck, J.; Percec, V. *Am. Chem. Soc. Div. Polym. Chem., Polym. Prepr.* **1991**, *32(1)*, 263. (c) Percec, V.; Heck, J. *Am. Chem. Soc. Div. Polym. Chem., Polym. Prepr.* **1991**, *32(3)*, 698. (d) Percec, V.; Heck, J. *J. Polym. Sci.: Part A: Polym. Chem.* **1991**, *29*, 591. (e) Percec, V.; Heck, J. *Polym. Bull.* **1990**, *24*, 255. (f) Percec, V.; Heck, J. *Polym. Bull.* **1991**, *25*, 55 and 431. (g) Percec, V.; Heck, J.; Ungar, G. *Macromolecules* **1991,** *24*, 4957. (h) Percec, V.; Heck, J.; Ungar, G. *Am. Chem. Soc. Div. Polym. Chem., Polym. Prepr.* **1992**, *33(1)*, 152. (i) Percec, V.; Lee, M.; Heck, J.; Blackwell, H.; Ungar, G. Alvarez-Castillo, A. *J. Mater. Chem.* **1992**, *2*, 931. (j) Percec, V.; Heck, J.; Lee, M.; Ungar, G.; Alvarez-Castillo, A. *J. Mater. Chem.* **1992**, *2*, 1033. (k) References 16c,d,f. (l) Percec, V.; Schlueter, D.; Ronda, J. C.; Johansson, G.; Ungar, G.: Zhou, J. P. *Macromolecules* **1996**, *29*, 1464.

(18) For X-ray characterization of a more ordered hexagonal phase obtained from macromolecular and supramolecular dendrimers which provides a structural arrangement of the monodendrons in the column, see: (a) Kwon, Y. K.; Chvalun, S.; Schneider, A.-I.; Blackwell, J.; Percec, V.; Heck, J. A. *Macromolecules* **1994**, *27*, 6129. (b) Kwon, Y. K.; Danko, C.; Chvalun, S.; Blackwell, J.; Heck, J. A.; Percec, V. *Macromol. Symp.* **1994**, *87*, 103. (c) Kwon, Y. K.; Chvalun, S. N.; Blackwell, J.; Percec, V.; Heck, J. A. *Macromolecules* **1995**, *28*, 1552.

(19) For some brief reviews on the design of macromolecular and supramolecular rod-like architectures obtained from tapered and conformationally flexible rod-like building blocks, see: (a) Percec, V.; Heck, J.; Johansson, G.; Tomazos, D.; Ungar, G. *Macromol. Symp.* **1994**, *77*, 237. (b) Percec, V.; Heck, J.; Johansson, G.; Tomazos, D.; Kawasumi, M.; Ungar, G. *J. Macromol. Sci.:-Pure Appl. Chem.* **1994**, *A31*, 1031. (c) Percec, V.; Heck, J.; Johansson, G.; Tomazos, D.; Kawasumi, M.; Chu, P.; Ungar, G. *Mol. Cryst. Liq. Cryst.* **1994**, *254*, 137. (d) Percec, V.; Heck, J.; Johansson, G.; Tomazos, D.; Kawasumi, M.; Chu, P.; Ungar, G. *J. Macromol. Sci.:-Pure Appl. Chem.* **1994**, *A31*, 1719. (e) Percec, V.; Johansson, G. *Macromol. Symp.* **1995**, *96*, 173. (f) Percec, V. *Pure Appl. Chem.* **1995**, *67*, 2031. (g) Percec, V.; Johansson, G.; Schlueter, D.; Ronda, J. C.; Ungar, G. *Macromol. Symp.* **1996**, *101*, 43.

(20) For a few fundamental publications on fluorinated materials, see: (a) Smart, B. E. In *Organofluorine Chemistry: Principles and Commercial Applications*; Banks, R. E., Smart, B. E., Tatlow, J. C., Eds.; Plenum: New York, 1994; p 57. (b) Feiring, A. E. *J. Macromol. Sci.:-Pure Appl. Chem.* **1994**, *A31*, 1657. (c) Eaton, D. F.; Smart, B. E. *J. Am. Chem. Soc.* **1990**, *112*, 2821. (d) Bunn, C. W.; Howells, E. R. *Nature* **1954**, *174*, 549.

(21) For examples on the stabilization of thermotropic LC phases by replacing perhydrogenated with perfluorinated segments: (a) Tournilhac, F.; Bosio, L.; Nicoud, J. F.; Simon, J. *Chem. Phys. Lett.* **1988**, *145*, 452. (b) Koden, M.; Nakagawa, K.; Ishii, Y.; Funada, S.; Matsuura, M.; Awani, K. *Mol. Cryst. Liq. Cryst. Lett.* **1989**, *6*, 285. (c) Nguyen, H. T.; Sigaud, G.; Achard, M. F.; Hardouin, F.; Tweig, R. J.; Betterton, K. *Liq. Cryst.* **1991**, *10*, 389. (d) Chiang, Y. H.; Ames, A. E.; Gaudiana, R. H.; Adams, T. G. *Mol. Cryst. Liq. Cryst.* **1991**, *208*, 85. (e) Takenaka, S. *J. Chem. Soc., Chem. Commun.* **1992**, 1748. (f) Pugh, C.; Arehart, S.; Liu, H.; Warayanan, R. *J. Macromol. Sci.-Pure Appl. Chem.* **1994**, *A31*, 1591. (g) Johansson, G.; Percec, V.; Ungar, G.; Smith, K. *Chem. Mater.*, in press.

(22) For representative publications on thermotropic liquid crystal phases from semifluorinated alkanes, see: (a) Mahler, W.; Guillon, D.; Skoulios, A. *Mol. Cryst. Liq. Cryst. Lett.* **1985**, *2*, 111. (b) Viney, C.; Twieg, R. J.; Gordon, B. R.; Rabolt, J. F. *Mol. Cryst. Liq. Cryst.* **1991**, *198*, 285. (c) Höpken, J.; Pugh, C.; Richtering, W.; Möller, M. *Makromol. Chem.* **1988**, *189*, 911. (d) Höpken, J.; Faulstich, S.; Möller, M. *Mol. Cryst. Liq. Cryst.* **1992**, *210*, 59.

(23) For selected examples of thermotropic mesophases formed from semifluorinated polymers, see: (a) Wilson, L. M.; Griffin, A. C. *Macromolecules* **1993**, *26*, 6212. (b) Davidson, T.; Griffin, A. C.; Wilson, L. M.; Windl, A. H. *Macromolecules* **1995**, *28*, 354. (c) Jariwala, C. P.; Mathias, L. J. *Macromolecules* **1993**, *26*, 5129. (d) Hoyle, C. E.; Kang, D.; Jariwala, C.; Griffin, A. C. *Polymer* **1993**, *34*, 3070. (e) Wilson, L. M. *Liq. Cryst.* **1994**, *17*, 277. (f) Wilson, L. M.; Griffin, A. C. *Macromolecules* **1994**, *27*, 1921. (g) Wilson, L. M.; Griffin, A. C. *Macromolecules* **1994**, *27*, 4611. (h) Wilson, L. M. *Macromolecules* **1995**, *28*, 347. (i) Wilson, L. M. *Liq. Cryst.* **1995**, *18*, 347. (j) Ref 21f.

(24) For selected publications on lyotropic systems from semifluorinated compounds, see: (a) Elbert, R.; Folda, T.; Ringsdorf, H. *J. Am. Chem. Soc.* **1984**, *106*, 7687. (b) Turberg, M. P.; Brady, J. E. *J. Am. Chem. Soc.* **1988**, *110*, 7797. (c) Kawahara, H.; Hamada, M.; Ishikawa, Y.; Kunitake, T. *J. Am. Chem. Soc.* **1993**, *115*, 3002. (d) Ishikawa, Y.; Kuwahara, H.; Kunitake, T. J. *J. Am. Chem. Soc.* **1989**, *111*, 8530. (e) Giulieri, F.; Krafft, M. P.; Riess, J. G. *Angew. Chem., Int. Ed. Engl.* **1994**, *33*, 1514.

(25) (a) Johansson, G.; Schlueter, D.; Percec, V. *Abstracts of the 35th IUPAC International Symposium on Macromolecules* **1994**, 354. (b) Percec, V.; Schlueter, D.; Kwon, Y. K.; Blackwell, J.; Möller, M.; Slangen, P. J. *Macromolecules* **1995**, *28*, 8807.

(26) Johansson, G.; Percec, V.; Ungar, G.; Zhou, J. P. *Macromolecules* **1996**, *29*, 646.

(27) Dahn, U.; Erdelen, C.; Ringsdorf, H.; Festag, R.; Wendorff, J. H.; Heiney, P. A.; Maliszewskyj, N. C. *Liq. Cryst.* **1995**, *19*, 759.

**Scheme 1.** Schematic Representation of the Self-Assembly of Tapered Building Blocks into a Supramolecular Columnar Architecture

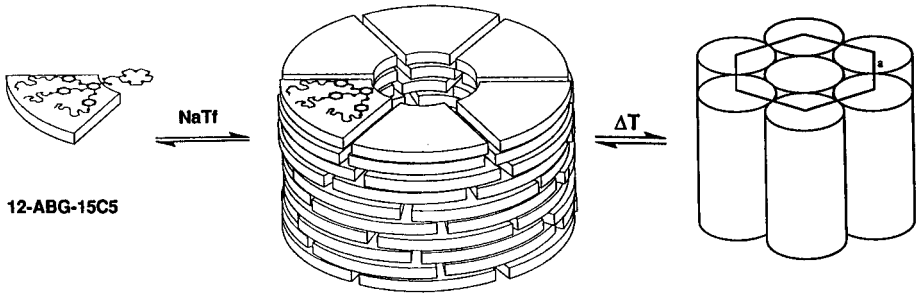


**Scheme 2.** Synthesis of **12Fn-AG-15C5** (**4-m/n**) and **12F8-AG-B15C5** (**5-4/8**)

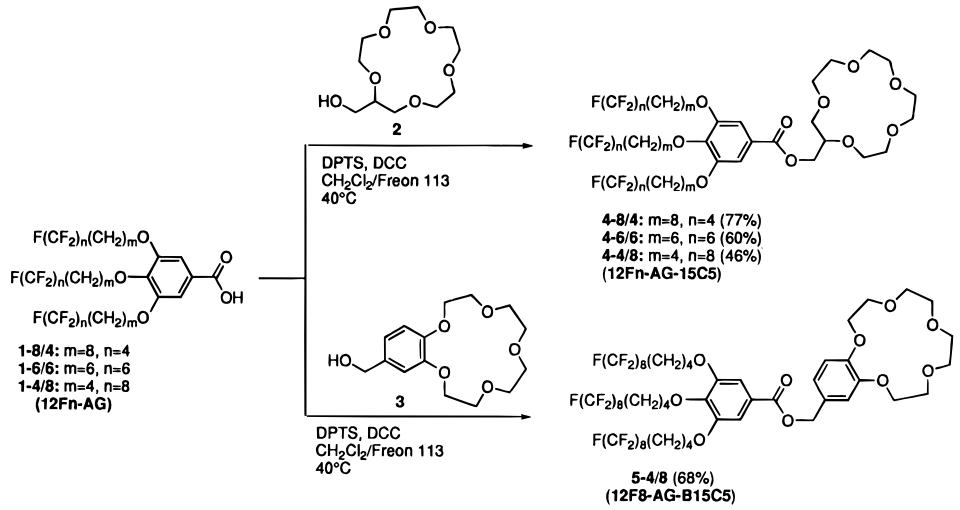


**Scheme 3.** Synthesis of **12F8-ABG-15C5** (**14-4/8**) and **12F8-ABG-B15C5** (**15-4/8**)

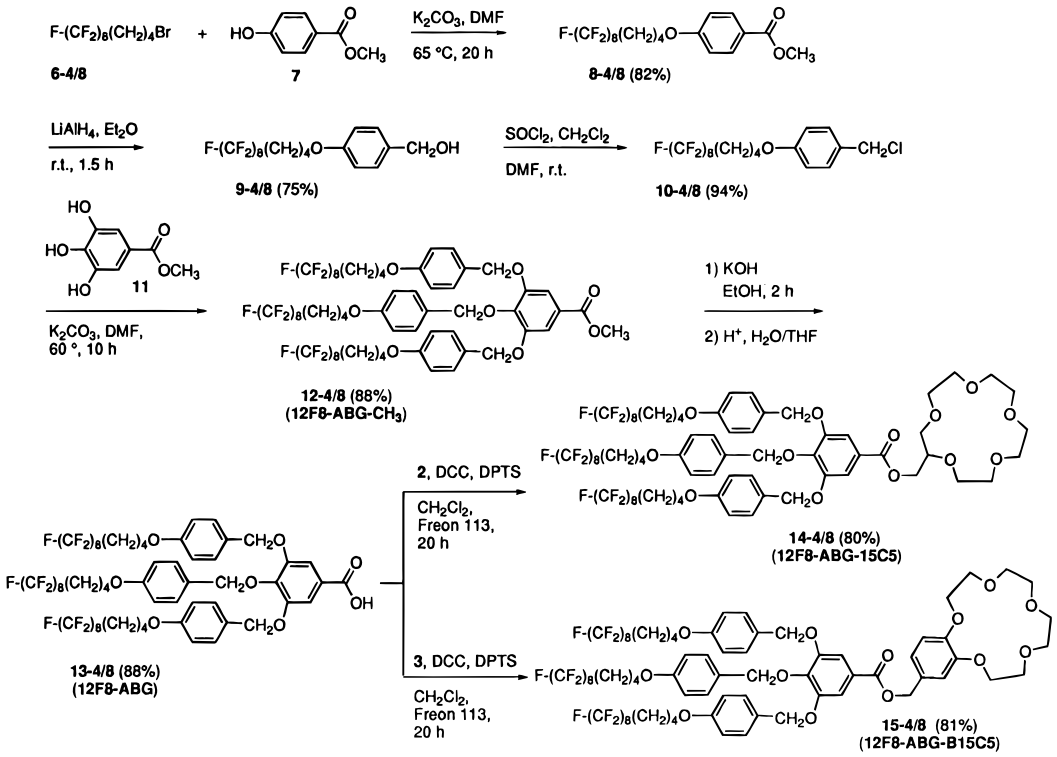


process. The evolution of this self-assembling process is estimated and analyzed by comparing the thermodynamic parameters of the $\Phi_h$ phase generated from supramolecular columns as a function of MOTf used in the complexation process with established theoretical and experimental dependencies of various parameters of thermodynamically controlled phase transitions *versus* degree of polymerization (i.e., first order transition temperatures, their corresponding enthalpy and entropy changes, and glass transition temperatures).[29−31] These experi-

(28) (a) deGennes, P. G.; Prost, J. *The Physics of Liqud Crystals*; Oxford University Press: Oxford, 1993. (b) Chandrasekhar, S. *Liquid Crystals*, 2nd ed.; Cambridge University Press: 1992.

ments have demonstrated a similar behavior for the supramolecular polymer "backbone" generated *via* ion-mediated interactions with that of covalent polymer backbones.[19a,e,f] When the crown ether of these building blocks was replaced with oligooxyethylenic segments containing a terminal -OH group which induces H-bonding interactions, the resulting **12-ABG-nEO-OH** self-assemble in the absence of ion complexation. In the absence of the H-bonding -OH group, the self-assembly process requires ion-complexation. Alternatively, the -OH group can be replaced with a polymer backbone to facilitate the self-assembly process.[16c,d,19a,e,f] **12-AG-nEO-OH** self-assemble only *via* an ion mediated recognition process or by replacing the -OH groups with a suitable polymer backbone.[16f,19a,f] Recently we discovered that semifluorination of the alkyl groups of **12-AG-nEO-OH** and of their corresponding polymers produces a dramatic stabilization of their $\Phi_h$ phase.[25] Subsequently, we discovered that a suitable length of the semifluorinated alkyl tail of **12-AG-nEO-OH** induces their self-assembly in the absence of ion complexation,[26] i.e., by a combination of the fluorophobic effect and H-bonding interactions. This last result prompted us to advance the hypothesis that a suitable semifluorination of the alkyl groups of **12-ABG-B15C5**, **12-ABG-15C5**, **12-AG-B15C5**, and **12-AG-15C5** may induce their self-assembly *via* the fluorophobic effect, and, therefore, this would have to occur in the absence of metal ion complexation or H-bonding processes.

Scheme 2 outlines the synthesis of **12Fn-AG-15C5** and **12F8-AG-B15C5** (where *n* and respectively 8 following the letter F indicates the number of fluorinated methylenic groups out of a total of 12). The synthesis of **12Fn-AG** with $n = 8$, 6, and 4 was reported previously.[26] The esterification of **12Fn-AG** with 1-hydroxymethyl(15-crown-5) (**2**)[16e] and 4′-hydroxymethylbenzo(15-crown-5) (**3**)[16b] was performed with DCC catalyzed by 4-dimethylaminopyridinium *p*-toluenesulfonate (DPTS),[16b] in $CH_2Cl_2$ when $n = 4$, 6 and in a mixture of $CH_2Cl_2$/Freon 113 (1:1 ratio) when $n = 8$. The yield of the esterification decreases with the increase of *n* due to the decreased solubility of the acylurea intermediate formed by the addition of **12Fn-AG** to DCC. The resulted building blocks were purified by flash column chromatography ($SiO_2$, $CHCl_3$/MeOH gradient) to more than 99% purities (HPLC, single spot TLC).

Scheme 3 describes the synthesis of **12F8-ABG-15C5** and **12F8-ABG-B15C5**. 4-Hydroxymethylbenzoate (**7**) was alkylated (DMF/$K_2CO_3$) with *n*-5,5,6,6,7,7,8,8,9,9,10,10,11,11,12,-12,12-heptadecafluorododecyl bromide (**6-4/8**) which was synthesized as reported previously[26] at 65 °C to produce **8-4/8** in 82% yield after 20 h. Reduction of **8-4/8** with $LiAlH_4$ in $Et_2O$ (room temperature, 1.5 h) yielded **9-4/8** (75% yield) which was chlorinated with $SOCl_2$ ($CH_2Cl_2$, DMF catalyst, room temperature) to produce **10-4/8** in 94% yield. Alkylation of methyl gallate with **10-4/8** by using standard conditions (DMF/$K_2CO_3$, 60 °C, 10 h) produced **12-4/8** (88% yield) (i.e., **12F8-ABG-CH₃**) which upon hydrolysis with KOH in EtOH (reflux, 2 h), neutralization with 10% HCl in THF and recrystallization from acetone produced **13-4/8** (**12F8-ABG**) in 88% yield. Esterification of **12F8-ABG** with **2** and respectively **3** [DCC/DPTS in $CH_2Cl_2$/Freon 113 (1:1)] produced **12F8-ABG-15C5** (80% yield) and respectively **12F8-ABG-B15C5** (81% yield). **12F8-ABG-15C5** was purified by flash column chromatography ($SiO_2$, $CHCl_3$/MeOH gradient), and **12F8-ABG-B15C5** was recrystallized from acetone to give products of more than 99% purities (HPLC, TLC).

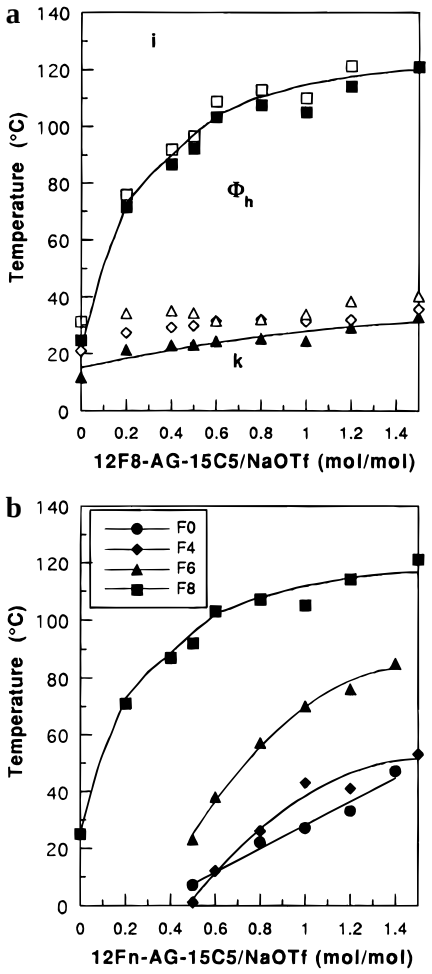


**Figure 1.** (a) The dependence of the transition temperatures of the complexes of **12F8-AG-15C5** with NaOTf on the NaOTf/**12F8-AG-15C5** molar ratio (a) from the second heating scan: ◇ $T_{k_1-k_2}$; △ $T_{k_2-\Phi_h}$; □ $T_i$; (b) from the cooling scan: ■ $T_{i-\Phi_h}$; ▲ $T_{\Phi_h-k}$. (b) The dependence of the i-$\Phi_h$ transition temperatures of the complexes of **12Fn-AG-15C5** with NaOTf on the NaOTf/**12Fn-AG-15C5** molar ratio: ● F0; ◆ F4; ▲ F6; ■ F8.

**Thermal Characterization.** The self-assembling process of these semifluorinated building blocks was investigated by a combination of techniques consisting of differential scanning calorimetry (DSC), thermal optical polarized microscopy, and X-ray diffraction experiments. When the building blocks self-assemble in the melt phase, they generate a columnar structure which produces the $\Phi_h$ LC phase which can be recognized and characterized by this combination of techniques. Figure 1 of Supporting Information shows selected heating and cooling DSC traces of various building blocks which self-assemble into supramolecular columns. The transition temperatures and the corresponding enthalpy changes of all compounds are summarized in Table 1. As we can observe from Figure 1a of Supporting Information, **12F8-AG-15C5** exhibits a crystalline

(29) For general reviews on main chain and side chain LC polymers which show different trends of phase transition temperatures-molecular weight dependence, see: (a) Percec, V.; Pugh, C. In *Side Chain Liquid Crystalline Polymers*; McArdle, C. B., Ed.; Chapman and Hall: New York, 1989; p 30. (b) Percec, V.; Tomazos, D. In *Comprehensive Polymer Science*, First. Suppl.; Allen, G., Ed.; Pergamon: Oxford, 1992; p 209. (c) Percec, V.; Tomazos, D. *Adv. Mater.* **1992**, *4*, 548. (d) Percec, V. In *Handbook of Liquid Crystal Research*; Collings, P. J., Patel, J. S., Eds.; Oxford University Press: Oxford, in press.

(30) For thermodynamic schemes which explain the dependence of liquid crystalline and crystalline transitions on molecular weight, see: (a) Percec, V.; Keller, A. *Macromolecules* **1990**, *23*, 4347. (b) Keller, A.; Ungar, G.; Percec, V. In *Advances in Liquid Crystalline Polymers*; Weiss, R. A., Ober, C. K., Eds.; ACS Symposium Series 435; American Chemical Society: Washington, DC, 1990; p 308.

(31) For the dependence of thermodynamic parameters of phase transitions on molecular weight in liquid crystal polymers, see: (side chain) (a) Percec, V.; Tomazos, D.; Pugh, C. *Macromolecules* **1989**, *22*, 3259. (main chain) (b) Percec, V.; Nava, H.; Jonsson, H. *J. Polym. Sci., Polym. Chem. Ed.* **1987**, *25*, 1943. (c) Percec, V.; Kawasumi, M. *Macromolecules* **1993**, *26*, 3663.

**Table 1.** Thermal Characterization of Semifluorinated Building Blocks and Selected Intermediary Compounds

| compd | phase transitions (°C) and corresponding enthalpy changes (kcal/mol)[a] heating | cooling |
|---|---|---|
| **12-AG-15C5**[16e] | k 32 (24.5) i<br>k 7 (12.8) −k 16 (5.66)<br>k 32 (6.81) i | i −8 (13.3) k |
| **12F4-AG-15C5** | k −35 (0.90) i<br>k −35 (1.36) i | i −41 (1.45) k |
| **12F6-AG-15C5** | k −5 (2.35) i<br>k −5 (2.66) i | i −14 (2.32) k |
| **12F8-AG-15C5** | k 46 (13.0) k 67 (1.83) i<br>k 21 (4.58) $\Phi_h$ 31 (0.30) i | i 25 (0.29) $\Phi_h$<br>12 (4.46) k |
| **12-AG-B15C5**[19e] | k 30 (0.90) k 88 (21.2) i<br>k 85 (20.1) i | i 55 (19.8)<br>k 15 (2.08) k |
| **12F8-AG-B15C5** | k 37 (1.75) −k 49 (0.85)<br>k 68 (5.26) $\Phi_h$ 78 (0.31) i<br>g 14 $\Phi_h$ 78 (0.26) i | i 74 (0.25) $\Phi_h$ 0 g |
| **12-ABG-CH$_3$**[16b] | k 67 (13.8) i[b] | i 37 (15.7) k |
| **12F8-ABG-CH$_3$** | k 104 (11.4) $\Phi_h$ 144 (3.37) i<br>k 104 (10.1) $\Phi_h$ 144 (3.01) i | i 140 (3.02) $\Phi_h$ 81 k |
| **12-ABG**[16c] | k 71 (6.92) $\Phi_h$ 143 (3.1) i[c] | i 137 (3.0)<br>$\Phi_h$ 51 (6.9) k |
| **12F8-ABG** | k 87 (6.56) $\Phi_h$ 203[d] | |
| **12-ABG-15C5**[16e] | k 60 (18.3) i<br>k 45 (16.0) i | i 12 (15.4) k |
| **12F8-ABG-15C5** | k 56 (6.19) $\Phi_h$ 135 (0.82) i<br>k 36 (1.06) k 69 (3.08) $\Phi_h$<br>135 (0.86) i | i 132 (0.83)<br>$\Phi_h$ 30 (4.27) k |
| **12-ABG-B15C5**[16b] | k 96 (19.3) i<br>k 50 −k 66−80 (3.47)<br>k 94 (15.9) i | i 34 (12.5) k |
| **12F8-ABG-B15C5** | k 63 (2.12) −k 85 (7.36)<br>k 125 (15.2) i<br>g 27 −k 76 (12.1)<br>k 125 (15.0) i | i 112 (0.32)<br>Cu 108 (0.05) 20 g |

[a] Data on the first line under cooling and heating are from the first scans. Data on the second line under heating are determined during the second heating scan. [b] Obtained during the second heating scan, lit.[32] mp, 65.5 °C. [c] Obtained during the second heating scan. [d] Sample decomposed during the first heating scan.

phase which melts and recrystallizes into a second crystalline phase, followed by isotropization at 67 °C. On subsequent cooling and heating scans this compound exhibits a narrow $\Phi_h$ phase (from 21 °C to 31 °C on heating and from 25 °C to 12 °C on cooling). The replacement of **15C5** with **B15C5** yields compound **12F8-AG-B15C5** which exhibits a melting into a $\Phi_h$ phase followed by isotropization in the first heating scan. The following cooling and heating scans show a very broad enantiotropic $\Phi_h$ phase from 74 °C to $T_g$ = 0 °C on cooling and from $T_g$ = 14 °C to $T_i$ = 78 °C on heating. These two results are extremely rewarding considering that **12-AG-15C5**,[16e] **12-AG-B15C5**,[19e] **12F4-AG-15C5**, and **12F6-AG-15C5** are only crystalline compounds (Table 1). The thermodynamic control of this self-assembling process can be assessed by observing the extremely low degree of supercooling (4 °C) and the almost identical enthalpy change (0.26 kcal/mol on heating *vs* 0.25 kcal/mol on cooling) associated with the isotropization temperature of the $\Phi_h$ phase (Table 1) of **12F8-AG-B15C5**. The transition from building blocks based on **12F8-AG** to building blocks based on **12F8-ABG** demonstrates an expected increase in the stability of the $\Phi_h$ phase obtained by the self-assembly *via* the fluorophobic effect. **12F8-ABG-CH$_3$** (Figure 1a, Supporting Information) exhibits an enantiotropic $\Phi_h$ phase which is stable over a broad range of temperature (Table 1), while the corresponding **12-ABG-CH$_3$** is crystalline (mp = 67 °C). Very instructive is to compare the stability of the $\Phi_h$ phase generated from **12F8-ABG** *versus* that of **12-ABG**. On the first DSC scan, **12F8-ABG** shows a melting at 87 °C into a $\Phi_h$ phase (Figure 1b, Supporting Information) which undergoes isotropization simultaneous with decomposition at 203 °C. The $\Phi_h$ phase of **12-ABG** is stable only up to 143 °C.[16c,32] We should mention that **12-ABG** and **12F8-ABG** form columnar structures by the dimerization of their carboxylic acid *via* H-bonding. Therefore, a direct comparison of these two $\Phi_h$ phases permits the determination of the contribution of the fluorophobic effect to the stabilization of this column which is of about 60 °C. Simultaneously, if we compare the stability of the $\Phi_h$ phase of **12F8-ABG** ($T_i$ = 203 °C) with that of **12F8-ABG-CH$_3$** ($T_i$ = 144 °C) we find out that the contribution of two H-bonds to the stabilization of this column is 59 °C, i.e., almost identical to that of the fluorophobic effect. Extremely interesting is that **12F8-ABG-15C5** shows a $\Phi_h$ phase up to 135 °C, while **12F8-ABG-B15C5** is only crystalline on heating and exhibits a cubic phase on cooling. This trend is the reverse of that observed for the homologous **12F8-AG** compounds. The formation of a cubic phase is associated with a change in the shape of the building block from tapered to conic, and this will be discussed in a different publication.

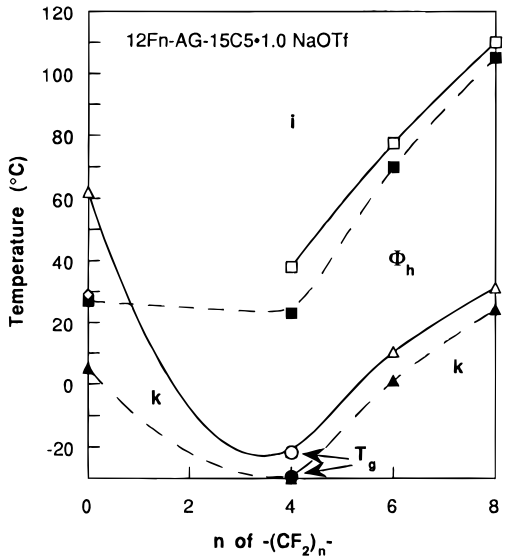


**Figure 2.** The dependence of the transition temperatures of the complexes of **12Fn-AG-15C5** with 1.0 equiv NaOTf on the number of fluorinated methylenes in the alkyl tails (*n*). Data from the cooling scan: ■ $T_{i-\Phi_h}$; ▲ $T_{\Phi_h-k}$; ● $T_g$. Data from the second heating scan: ◇ $T_{k-k}$; ○ $T_g$; △ $T_{k-\Phi_h}$; □ $T_{\Phi_h-i}$.

**Characterization by Optical Polarized Microscopy.** On the optical polarized microscope, the $\Phi_h$ phase generated from supramolecular columns displays identical textures as the similar columnar LC phases obtained from discotic liquid crystals.[28b,33] Figure 2a (Supporting Information) presents the texture exhibited by the $\Phi_h$ phase of **12F8-AG-15C5**. The sample was sandwiched between untreated glass slides and cooled at 0.1 °C·min$^{-1}$ from the isotropic melt. The texture is characterized by several large fans surrounded by large homeotropic domains. However on shearing, the texture becomes highly birefringent. In the homeotropic alignment, the supramolecular columns are oriented with their cylindrical axes perpendicular to the substrate. Such a facile alignment in the absence of an externally applied magnetic or electric field is remarkable. A similar texture is observed for the $\Phi_h$ phase of **12F8-ABG-CH$_3$** (Figure 2b,

(32) Malthête, J.; Collet, A.; Levelut, A.-M. *Liq. Cryst.* **1989**, *5*, 123.
(33) For specific textures exhibited by columnar mesophases of discotic liquid crystals, see: (a) Percec, V.; Cho, C. G.; Pugh, C. *J. Mater. Chem.* **1991**, *1*, 217. (b) Percec, V.; Cho, C. G.; Pugh, C.; Tomazos, D. *Macromolecules* **1992**, *25*, 1164. (c) Serrette, A.; Lai, C. K.; Swager, T. M. *Chem. Mater.* **1994**, *6*, 2252. (d) Chandrasekhar, S.; Rangarath, G. S. *Rep. Prog. Phys.* **1990**, *53*, 57. (e) Destrade, C.; Foucher, P.; Gasparoux, H.; Tinh, N. H.; Levelut, A. M.; Malthête, J. *Mol. Cryst. Liq. Cryst.* **1984**, *106*, 121.

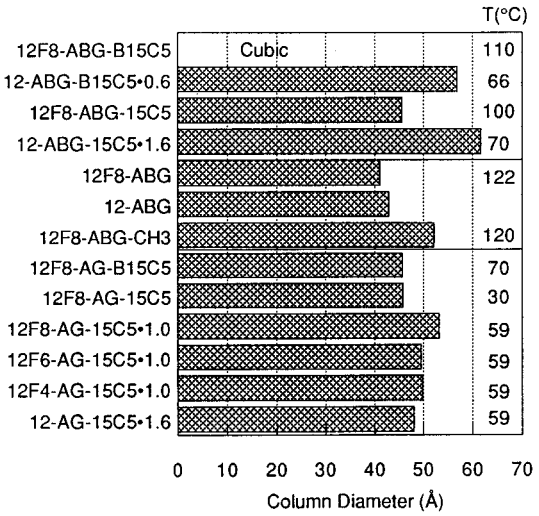


**Figure 3.** Comparison of the column diameter of the supramolecular columns (at the temperature indicated) obtained by the self-assembly of selected fluorinated and non-fluorinated compounds.

Supporting Information) and of other semifluorinated supramolecular columns. The $\Phi_h$ phase of 12F8-ABG-15C5 is homeotropically aligned over its entire temperature range. On shearing, faint birefringence is observed.

**Mechanism of Fluorophobic-Mediated Self-Assembly with the Aid of Ion-Mediated Self-Assembly.** The comparative investigation of self-assembly via ion-mediated, fluorophobic-mediated and by a combination of both allows the elucidation of the mechanism of self-assembly solely via fluorophobic effect. Ion-mediated self-assembly experiments were carried out for the series **12Fn-AG-15C5/NaOTf**. An example of DSC traces and a complete phase diagram are provided for the system **12F8-AG-15C5/NaOTf** in Figures 3 (Supporting Information) and 1a. An increase of the stability of the $\Phi_h$ phase is observed upon complexation with a very small amount of NaOTf. For example 0.2 mol of NaOTf per **12F8-AG-15C5** increases the stability of the $\Phi_h$ phase with 45 °C (Figure 3, Supporting Information). A continuous increase of the stability of this phase is observed with the increase in NaOTf until the limit of the complexation ability of **12F8-AG-15C5** is reached. Above this value, a plateau of the temperature transition is observed. Simultaneous with this trend, the melting temperature is increasing much less, and the rate of crystallization decreases.

A plot of the experimental data collected from Figure 3 (Supporting Information) is presented in Figure 1a. This plot can be inspected in two different ways. First it can be considered as a solid state titration experiment. The plateau of *T vs* **12F8-AG-15C5/NaOTf** (mol/mol) ratio provides the maximum amount of complexed NaOTf, which unexpectedly is larger than 1.0 mol of NaOTf per **15C5**. We should remember that the crown ether groups are packed side-by-side in the center of the column, and in the $\Phi_h$ phase they are melted. This means that the NaOTf is complexed both in the cavity of the crown ether with a very small amount being placed in between the melted crown ethers. The second way we should inspect this phase diagram is as a first order temperature transition dependence on molecular weight of a polymer. An increased amount of NaOTf complexed by the crown ether creates a "supramolecular" polymer with a higher molecular weight. Therefore, the ratio **12F8-AG-15C5/NaOTf** from Figure 1a can be envisioned as molecular weight or degree of polymerization. An inspection of Figure 1a from this point of view demonstrates a textbook like dependence of the isotropization and melting transition temperatures as a function of molecular weight.[29−31] Both the isotropization and the melting temperature should increase with the increase of molecular weight until they reach a plateau. However, since the slope of the $T_i$-$M_n$ is higher than that of $T_k$-$M_n$,[30,31] the thermal stability of the LC phase broadens *via* polymerization. In the case of LC polymers this trend is known as the "polymer effect".[29,30] By analogy with this nomenclature, we suggest the name "supramolecular polymer effect" for the case of the self-assembly of polymer-like structures *via* a supramolecular polymer backbone.

**Table 2.** Thermal Characterization of the 1:1 Complexes of **12Fn-A(B)G-(B)15C5** with **NaOTf**

| | phase transitions (°C) and corresponding enthalpy changes (kcal/mol)[a] | |
|---|---|---|
| compd | heating | cooling |
| **12-AG-15C5·1.0**[16e] | k 33 (0.32) k 69 (18.7) i<br>k 29 (7.79) −k 39 (12.6) k 62 (13.0) i | i 27 (0.06) $\Phi_h$ 5 (7.51) k |
| **12F4-AG-15C5·1.0** | g −22 $\Phi_h$ 50 (0.06) i<br>g −22 $\Phi_h$ 49 (0.04) i | i 43 (0.02) $\Phi_h$ −30 g |
| **12F6-AG-15C5·1.0** | k 11 (0.89) $\Phi_h$ 77 (0.06) i<br>k 10 (1.15) $\Phi_h$ 77 (0.06) i | i 70 (0.06) $\Phi_h$ 1 (1.01) k |
| **12F8-AG-15C5·1.0** | k 46 (4.69) $\Phi_h$ 110 (0.23) i<br>k 31 (1.25) $\Phi_h$ 110 (0.11) i | i 105 (0.11) $\Phi_h$ 24 (1.84) k |
| **12-AG-B15C5·1.0**[19e] | k 45 (−) $\Phi_h$ 62 (12.1)[b] i<br>g 13 $\Phi_h$ 66 (0.05) i | i 54 (0.04) $\Phi_h$ −4 g |
| **12-ABG-15C5·1.0**[16e] | k 46 (14.3) $\Phi_h$ 94 (0.39) i<br>g 19 $\Phi_h$ 94 (0.17) i | i 84 (0.18) $\Phi_h$ 10 g |
| **12-ABG-B15C5·1.0**[16b] | g 38 $\Phi_h$ 107 (0.51) i<br>g 41 $\Phi_h$ 106 (0.24) i | i 98 (0.24) $\Phi_h$ 31 g |

[a] Data on the first line under cooling and heating are from the first scans. Data on the second line under heating are determined during the second heating scan. [b] Sum of overlapped transition enthalpies.

Figure 1b plots the dependence of the isotropic-$\Phi_h$ temperature transition on **12Fn-AG-15C5/NaOTf** (mol/mol) ratio for $n = 0$, 4, 6, and 8. The DSC figures, plots, and tables with complete experimental data are available as supporting information. A similar trend is observed for the entire set of semifluorinated tapered groups. The increase in the extent of fluorination shifts this dependence to higher temperatures. The entire set of transition temperatures (i.e., $\Phi_h$-isotropic (i); i-$\Phi_h$, melting, crystallization, and $T_g$) of **12Fn-AG-15C5/NaOTf** = 1/1 collected from these diagrams is summarized in Table 2 and plotted in Figure 2 as a function of *n*. This "phase diagram" shows a eutectic composition for melting and crystallization and a continuous dependence of the $\Phi_h$-i temperature on *n*. These two dissimilar trends explain the fluorophobic effect in this self-assembly process. From $n = 0-4$, there is a small increase in the stability of the $\Phi_h$ and a dramatic destabilization of the crystalline phase. As a consequence, even such a very small amount of semifluorination increases dramatically the ability of these building blocks toward self-assembly. From $n = 4$ to 8 both $\Phi_h$-i and melting transition temperatures increase with a slightly higher slope for the former. As a consequence, at $n = 8$ the melting temperature does not recover up to the parent value of $n = 0$, while the $\Phi_h$-i transition temperature increases with another 60 °C. *At this point, ion mediated self-assembly can be replaced completely by the fluorophobic effect.*

The bar graph in Figure 10 (Supporting Information) provides a direct comparison of the thermal stability of the various phases displayed by the most representative building blocks and of some of their 1:1 complexes with NaOTf as reported in Tables 1 and 2. The following remarkable conclusion is obtained from these data. **12F8-AG-15C5** shows a broader temperature range for its $\Phi_h$ phase than **12-AG-15C5·1.0**. The suffix 1.0 refers to the amount of NaOTf in the corresponding complex. However, the thermal stability of the $\Phi_h$ phase of the latter is lower than of its semifluorinated partner. In both **12-AG-**

**Table 3.** Characterization of **12Fn-AG-15C5**, **12Fn-AG-B15C5**, **12Fn-ABG**, **12F8-ABG-CH$_3$**, **12Fn-ABG-15C5**, and **12Fn-ABG-B15C5** by Small-Angle X-ray Scattering

| entry | NaOTf (equiv) | $T$ (°C) | $d_{100}$ (Å) | $d_{110}$ (Å) | $d_{200}$ (Å) | $d_{210}$ (Å) | $d_{300}$ (Å) | $\langle d_{100}\rangle^a$ (Å) | $a^b$ (Å) | $R^c$ (Å) | $S^d$ (Å) | $\rho^e$ (g/cc) | $\mu^f$ |
|---|---|---|---|---|---|---|---|---|---|---|---|---|---|
| **12-AG-15C5** | 1.6 | 59 | 42.1 | | 20.6 | | | 41.7 | 48.1 | 24.1 | 27.8 | 1.12 | 4.36 |
| **12F4-AG-15C5** | 1.0 | 29 | 41.8 | 24.1 | 21.0 | 15.9 | | 41.9 | 48.4 | 24.2 | 27.9 | 1.25 | 3.70 |
| **12F4-AG-15C5** | 1.0 | 39 | 42.1 | 24.5 | | 15.8 | | 42.1 | 48.6 | 24.3 | 28.1 | | |
| **12F4-AG-15C5** | 1.0 | 59[g] | | | | | | 43.1 | 49.8 | 24.9 | 28.7 | | |
| **12F6-AG-15C5** | 1.0 | 28 | 43.0 | 25.3 | 21.9 | 16.6 | | 43.6 | 50.3 | 25.2 | 29.0 | 1.41 | 3.96 |
| **12F6-AG-15C5** | 1.0 | 59 | 42.7 | 24.7 | 21.6 | | | 42.9 | 49.5 | 24.8 | 28.6 | | |
| **12F8-AG-15C5** | 0 | 30 | 39.5 | | 23.0 | | | 39.7 | 45.8 | 22.9 | 26.5 | 1.55 | 3.54 |
| **12F8-AG-15C5** | 1.0 | 59 | 46.1 | | 23.0 | | | 46.1 | 53.2 | 26.6 | 30.7 | 1.54 | 4.32 |
| **12F8-AG-15C5** | 1.0 | 80 | 44.7 | | 22.5 | | | 44.9 | 51.8 | 25.9 | 29.9 | 1.54 | 4.10 |
| **12F8-AG-B15C5** | 0 | 70 | 39.7 | | 19.8 | 14.9 | | 39.6 | 45.7 | 22.9 | 26.4 | 1.63 | 3.61 |
| **12F8-ABG-CH3** | 0 | 120 | 45.0 | | 22.5 | 17.2 | 14.9 | 45.2 | 52.2 | 26.1 | 30.1 | 1.63 | 4.40 |
| **12-ABG** | 0 | | | | | | | | 42.9[h] | 21.5 | 24.8 | | |
| **12F8-ABG** | 0 | 122 | 35.7 | 20.5 | 18.0 | 13.3 | | 35.6 | 41.1 | 20.6 | 23.7 | 1.63 | 2.85 |
| **12-ABG-15C5** | 1.6 | 70 | 52.9 | 31.8 | 26.2 | | | 53.5 | 61.7 | 30.9 | 35.6 | 1.15 | 5.71 |
| **12F8-ABG-15C5** | 0 | 100 | 40.3 | | 19.7 | 14.7 | 13.2 | 39.5 | 45.6 | 22.8 | 26.3 | 1.62 | 3.11 |
| **12-ABG-B15C5** | 0.6 | 66 | 49.0 | 28.1 | 25.1 | | | 49.3 | 56.9 | 28.5 | 32.9 | 1.09 | 5.09 |
| **12F8-ABG-B15C5** | 0 | 110 | | | | | | cubic | | | | 1.57 | |

[a] $\langle d_{100}\rangle = (d_{100} + \sqrt{3}\cdot d_{110} + \sqrt{4}\cdot d_{200} + \sqrt{7}\cdot d_{210} + \sqrt{9}\cdot d_{300})/5$. [b] $a = 2\langle d_{100}\rangle/\sqrt{3}$. [c] $R = \langle d_{100}\rangle/\sqrt{3}$. [d] $S = 2R/\sqrt{3}$. [e] Densities were measured at 20 °C. [f] Values of $\mu$ are based on a layer thickness, $t$, of 3.74 Å. [g] Extrapolated value. [h] From ref 32.

**B15C5·1.0/12F8-AG-B15C5** and **12-ABG-15C5·1.0/12F8-ABG-15C5** pairs the range of the stability of the $\Phi_h$ phase and its isotropization temperature are higher for the fluorinated compound.

**Characterization by X-ray Diffraction Demonstrates the Control of Column Diameter *via* Ion-Complexation and Flourination.** Table 3 summarizes the results of small angle X-ray diffraction experiments on the series of semifluorinated building blocks. Analysis was carried out on unoriented samples in glass capillaries mounted in a temperature controlled cell. Short exposures were obtained after slow cooling (<1 °C min$^{-1}$) from the isotropic melt to the temperature of interest within the $\Phi_h$ phase. Most of the compounds displayed at least three or more reflections characteristic of the $\Phi_h$ LC phase with Bragg spacings in the ratio of $d_{100}$:$d_{110}$:$d_{200}$:$d_{210}$:$d_{300}$ = 1:(1/$\sqrt{3}$):(1/$\sqrt{4}$): (1/$\sqrt{7}$):(1/$\sqrt{9}$).[16b] The intensities were of the order of $d_{100} > d_{110} > d_{210}$ for the nonfluorinated compounds and $d_{100} > d_{210} > d_{110}$ for the semifluorinated compounds. This inversion is due to the higher electron density present in the semifluorinated alkyl tails.[25,26] The hexagonal lattice parameter ($a = 2\langle d_{100}\rangle/\sqrt{3}$) is equal to the diameter of the self-assembled column which is responsible for the generation of the $\Phi_h$ phase as shown in Scheme 1. Values for the radius ($R = a/2$) and the hexagonal side length ($S = 2R/\sqrt{3}$) are also reported in Table 3.

The bar graph in Figure 3 provides a comparison of the diameter of the supramolecular columns formed from various nonfluorinated and semifluorinated building blocks. Strict comparisons of column diameters of supramolecular columns formed from various tapered building blocks are difficult to obtain due to the nonlinear contraction of the columnar lattice parameter with increasing temperature.[18] For the series, **12Fn-AG-15C5·1.0**, the diameter of the columns was found to increase with increasing the value of *n*. These values range from 48.1 Å for $n = 0$ (**12-AG-15C5·1.6**) to 53.2 Å for $n = 8$ (**12F8-AG-15C5·1.0**). One factor that can account for the overall increase is the larger -$CF_2CF_2$- bond length (1.58 Å) compared to -$CH_2CH_2$- (1.54 Å). A similar analysis for compounds where oligooxyethylenic units were used in place of the crown ether moieties showed that based on molecular models, the marginal increase (+0.7 Å) in the alkyl tail length could not accommodate the large increase in the column diameter with increasing *n*.[26] Therefore, we consider that other factors such as the increased rigidity and volume of the perfluoroalkane segments may contribute as well. The three local energy minima corresponding to two *gauche* and one *trans* conformer of decafluorobutane exist in a ratio of *trans*/*gauche* conformers of 95/5 due to the increased van der Waals radius of the fluorine atom.[21b] Therefore, fluorination increases both the linearity and the rigidity of the perfluoroalkane segments. This may be the major contributing factor to the increase in the column diameter with increasing *n*.

The effect of ion complexation on the column diameter is exemplified by comparing **12F8-AG-15C5** and **12F8-AG-15C5·1.0** (Figure 3). Complexation of **12F8-AG-15C5** with 1.0 mol NaOTf results in an increase in the column diameter from 45.8 to 51.8 Å. An even more striking example is provided by the comparison of **12-ABG-15C5·1.6** (1.6 mol NaOTf/**15C5**) with **12F8-ABG-15C5**. The former has a column diameter of 61.7 Å *versus* 45.6 Å for **12F8-ABG-15C5**. Therefore, the resulting complex must accommodate both the cation and the bulky triflate counteranion within the columnar structure resulting in this expansion of the column diameter. Similar results have been obtained from ABG-based complexes of nonfluorinated tapered building blocks containing an oligooxyethylenic ligand with LiOTf.[16c] The noncomplexed ABG-based tapered groups are self-assembled *via* H-bonding. The largest diameters are observed, as expected, for the complexes of **12-ABG-B15C5** and **12-ABG-15C5** which contain the combination of metal complexes in the column center and benzyl ether moieties in the alkyl tails.

To better understand the packing arrangement of the tapered building blocks within the supramolecular column, density measurements were obtained and the number, $\mu$, of tapered groups per column layer was calculated from $\mu = 3\sqrt{3}\rho N_A S^2 t/2M$,[16b] where $\rho$ is the density (g/Å$^3$), $N_A$ is Avogadro's number (6.022045 × 10$^{23}$ mol$^{-1}$), $S$ is the distance from the column center to the hexagonal vertex (Å), $t$ is the layer thickness (Å), and $M$ is the molar mass of the tapered building block. Experimentally determined values for $\rho$ and $S$ are reported in Table 3. Since all of our X-ray experiments have been conducted on unoriented samples in the $\Phi_h$ phase, we do not have any information about the repeat unit along the column. Therefore, the layer thickness, $t$, is taken as the average distance between adjacent benzene rings in the direction of the column axis (3.74 Å) as reported in the literature.[34] We have used this value consistently in reporting molecular arrangements within the layers of analogous supramolecular columns and retain it

(34) Safinya, C. R.; Liang, K. S.; Varady, W. A.; Clark, N. A.; Anderson, G. *Phys. Rev. Lett.* **1984**, *53*, 1172.

here for purposes of comparison. The calculated values for $\mu$ are reported in Table 3. Based on these values, the number of tapered building blocks per column stratum ranges from 3 to 6. Arrangements of the alkali metal complexes of the nonfluorinated entries, **12-AG-15C5**, **12-ABG-15C5**, and **12-ABG-B15C5** have been dicussed in detail,[16b,e] and their values of $\mu$ range from 4.4 to 5.7. Semifluorinated tapered building blocks self-assemble into columnar structures containing 3.1 to 4.4 structural units per stratum according to the data in Table 3. Notable exceptions are **12-ABG** and **12F8-ABG**. The former, as previously mentioned, exists as a H-bonded dimer in the column layer. It is therefore expected that **12F8-ABG** should have a similar packing arrangement. However, the calculated value of $\mu$ for **12F8-ABG** is 3.1. In order to obtain a model based on the H-bonded dimer, a layer thickness, *t*, of 5.82 Å would have to be assumed. The cross-sectional area occupied by hexagonally packed perfluoroalkanes (28.3 Å$^2$) has been reported in the literature.[35] Based on this value, a layer thickness, *t*, which is determined by the thickness of the perfluorinated segments of the alkyl tails can be calculated as 6.02 Å which is in good agreement with the dimer model. Therefore, the values of $\mu$ calculated for the semifluorinated tapered building blocks of Table 3 are most probably underestimated by ~35%. If the range of values is adjusted for the semifluorinated tapered building blocks, we find that 4.2 to 5.9 molecules pack within the column layer. This is in good agreement with the values reported for the complexes of **12-AG-15C5**, **12-ABG-15C5**, and **12-ABG-B15C5** with NaOTf in Table 3.

**Molecular Model of the Supramolecular Column.** Molecular models of the self-assembled supramolecular columns can be constructed based on the data discussed in the preceding sections. Figure 4a shows a space-filled molecular model of the top view of the self-assembled supramolecular column of the complex of **12F8-AG-15C5** with NaOTf. Five molecules of **12F8-AG-15C5** are arranged within a column stratum with the crown ethers arranged side-by-side in the center and the melted alkyl tails radiating toward the periphery of the column. The taper shaped structural units are situated in a close packed arrangement with disordered alkyl tails representative of the melt phase. Sodium cations are colored blue and are complexed within the cavity of the crown ether. Triflate counteranions are sandwiched between the layers and have been arbitrarily positioned in close proximity to the complexed metal atoms. The interlayer distance is 6 Å, and the column diameter is 50 Å. This view shows the microphase segregation of the perfluorinated and perhydrogenated/aromatic portions of the semifluorinated tapered building blocks in the $\Phi_h$ phase. A cross-section of the side-view for the same structure is shown in Figure 4b. The complexed metal cations are readily visible in the column center arrayed along the column axis. Since the column is packed in a liquid crystalline phase and three-dimensional order in this phase is absent both within the column and in between columns, we purposely show it in Figure 4 with some structural irregularities.

In conclusion, the results summarized in this paper have demonstrated the self-assembly of tapered monodendrons containing crown ethers into cylindrical or rod-like supramolecular dendrimers solely *via* the fluorophobic effect. Previously, similar cylindrical dendrimers were assembled *via* ion-mediated and H-bonding processes and by a combination of both or *via* the attachment of these building blocks to a suitable polymer backbone. This demonstration enlarges the already rich arsenal of molecular recognition processes used in self-assembly with the new and very powerful fluorophobic effect. We foresee

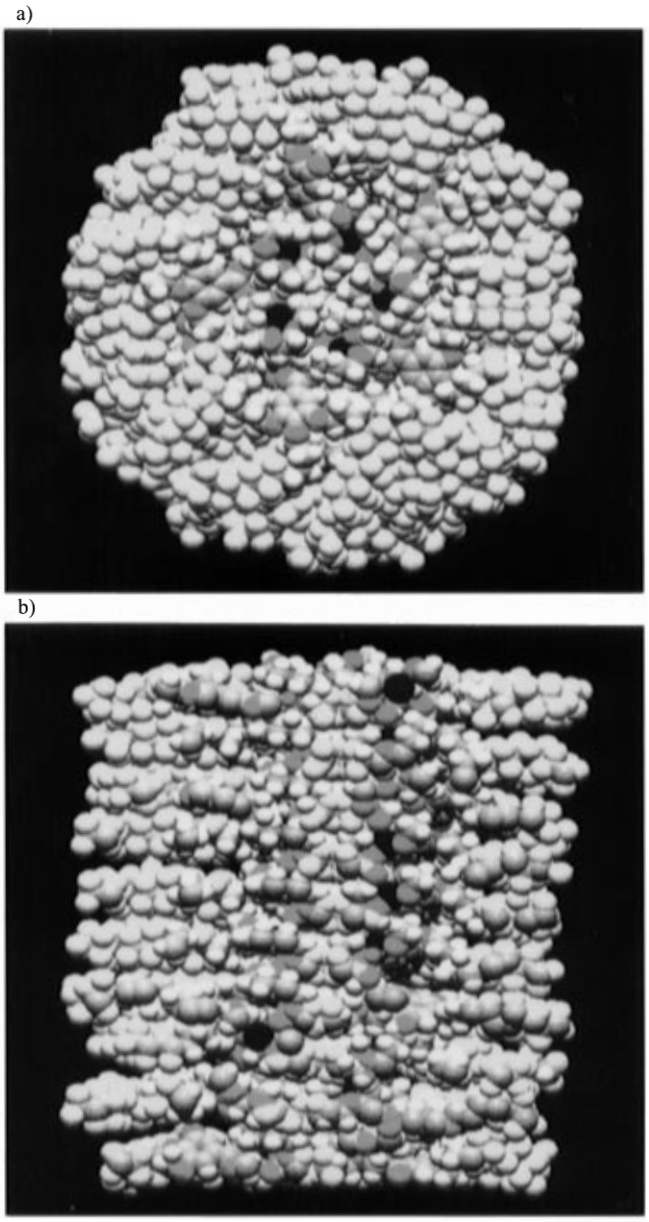


**Figure 4.** Space filled molecular model of the self-assembled supramolecular columnar structure of the complex of **12F8-AG-15C5** with NaOTf. (a) Top view and (b) cross-section of side view: F, yellow; O, red; S, yellow; H, white; C, gray.

the immediate application of this concept to self-assembly and/or stabilization of other related supramolecular systems.[36−39] These supramolecular semifluorinated columns assemble into a $\Phi_h$ liquid crystalline phase which aligns homeotropically, i.e., on untreated glass slides forms single crystal liquid crystals with the columns oriented with their long axes perpendicular to the glass surface. This is an extremely important result with implications in many technological applications such as, for example, in the design of one-dimensional membranes,[40] ionic[16bh,41,42] and electronic[43] conductors, photoconductors,[44] etc.

(35) (a) Höpken, J.; Möller, M. *Macromolecules* **1992**, *25*, 2482. (b) Dorset, D. L. *Chem. Phys. Lipids* **1977**, *20*, 13.

(36) (a) van Nunen, J. L. M.; Stevens, R. S. A.; Picken, S. J.; Nolte, R. J. M. *J. Am. Chem. Soc.* **1994**, *116*, 8826. (b) van Nunen, J. L. M.; Schenning, A. P. H. J.; Hafkamp, R. J. H.; van Nostrum, C. F.; Feiters, M. C.; Nolte, R. J. M. *Macromol. Symp.* **1995**, *98*, 483.

(37) (a) Fu, D. K.; Xu, B.; Swager, T. M. *J. Org. Chem.* **1996**, *61*, 802. (b) Xu, B.; Swager, T. M. *J. Am. Chem. Soc.* **1995**, *117*, 5011. (c) Zheng, H.; Swager, T. M. *J. Am. Chem. Soc.* **1994**, *116*, 761. (d) Serrette, A.-G.; Swager, T. M. *Angew. Chem., Int. Ed. Engl.* **1994**, *33*, 2342. (e) Serrette, A. G.; Swager, T. M. *J. Am. Chem. Soc.* **1993**, *115*, 8879. (f) Lai, C. K.; Serrette, A. G.; Swager, T. M. *J. Am. Chem. Soc.* **1992**, *114*, 7948.

(38) van Velzen, E. U. T.; Engbersen, J. F. J.; Reinhoudt, D. N. *J. Am. Chem. Soc.* **1994**, *116*, 3597.

(39) Kato, T.; Fréchet, J. M. J. *Macromol. Symp.* **1995**, *98*, 311.

The formation of single crystal liquid crystals from $\Phi_h$ mesophases is a very difficult process which so far was manipulated most efficiently by using a very high magnetic field[45a] or LC elastomers obtained from mesogens forming columnar mesophases.[45b] The LC phase of fluorinated systems show sharper phase transitions and lower viscosity.

Preliminary experiments have demonstrated that the crown ethers of these semifluorinated tapered groups can be replaced with a large number of other functionalities which become part of the core of these supramolecular columns (i.e., donors, acceptors, donor−acceptor complexes, nonlinear optical compounds, etc.). Last but not least, this self-assembly *via* fluorophobic effect, which is an amplified version of the hydrophobic effect, suggests that the hydrophobic effect alone should be able to generate a similar organizing force which is based on repulsive rather than attractive forces at the site of organization. The absence of strong attractive forces provides nonrigid self-assembled structures which are known to be uniquely suited for the first critical steps in the organization of living matter whose deformability is not only a virtue but very likely a necessity.[8b] Since the liquid crystalline state is a preorganized state of the crystalline phase,[46] this soft order[47] which is not generated *via* directed polar bonds should be as important in the assembly of synthetic systems as in the biological ones.

## Experimental Section

**Materials.** DCC (99%), DMAP (99%), methyl *p*-hydroxybenzoate (**7**) (99%), $LiAlH_4$ (95+%), $SOCl_2$ (99+%), and methyl 3,4,5-trihydroxybenzoate (**11**) (98%) (all from Aldrich) were used as received. *p*-TsOH and 1,1,2-trichloro-1,2,2-trifluoroethane (Freon 113) (all from Fisher Scientific) were used as received. THF (A.C.S. reagent, Fisher Scientific) was refluxed over sodium ketyl and distilled freshly before use. $CH_2Cl_2$ (Fisher) was dried by refluxing over $CaH_2$ and freshly distilled before use. DMF (Fisher, A.C.S. reagent) was used as received.

**General Methods.** $^1$H NMR (200 MHz), $^{19}$F NMR (188 MHz), and $^{13}$C NMR (50 MHz) spectra were recorded on a Varian Gemini 200 spectrometer. The purity of products was determined by a combination of TLC (single spot) on silica gel plates (Kodak) with fluorescent indicator and HPLC using a Perkin-Elmer Series 10 HPLC equipped with an LC-100 column oven, Nelson Analytical 900 Series integrator data station, and two Perkin-Elmer PL gel columns of $5 \times 10^2$ and $1 \times 10^4$ Å after the structure was confirmed by NMR and elemental analyses. Elemental analyses were carried out by Galbraith Laboratories. THF was used as solvent at the oven temperature of 40 °C unless otherwise noted. Detection was by UV absorbance at 254 nm. In some instances, purity was determined by GC using a Hewlett Packard 5890A gas chromatograph equipped with a Hewlett Packard 3392A integrator. A packed column consisting of 10% SP2100 on 80/100 Supelcoport stationary phase was used with a head pressure of 40−60 psi. The carrier gas was $N_2$.

Thermal transitions were measured on a Perkin Elmer DSC-7. In all cases, the heating and cooling rates were 10 °C min$^{-1}$ unless otherwise noted. First order transition temperatures were reported as the maxima and minima of their endothermic and exothermic peaks. Glass transition temperatures ($T_g$) were read at the middle of the change in heat capacity. Zn and In were used as calibration standards. An Olympus BX-40 optical polarized microscope (100× magnification) equipped with a Mettler FP 82 hot stage and a Mettler FP 80 central processor was used to verify thermal transitions and characterize anisotropic textures.

X-ray diffraction experiments on liquid crystal phases were performed using an Image Plate area detector (MAR Research) with a graphite-monochromatized pinhole-collimated beam and a helium tent. The samples, in glass capillaries, were held at constant temperature (±0.1 °C) in a temperature-controlled cell.

Macromodel 5.0 from Columbia Innovation Corp. was used on a Silicon Graphics Indy workstation to model the self-assembled supramolecular columnar structures.

**Synthesis.** The syntheses of 4-dimethylaminopyridinium *p*-toluenesulfonate (DPTS),[16b] 3,4,5-tris(*n*-dodecan-1-yloxy)benzoic acid (**1-12/0**),[16b] 3,4,5-tris(*n*-9,9,10,10,11,11,12,12,12-nonafluorododecan-1-yloxy)benzoic acid (**1-8/4**),[26] 3,4,5-tris(*n*-7,7,8,8,9,9,10,10,11,11,12,12,12-tridecafluorododecan-1-yloxy)benzoic acid (**1-6/6**),[26] 3,4,5-tris(*n*-5,5,6,6,7,7,8,8,9,9,10,10,11,11,12,12,12-heptadecafluorododecan-1-yloxy)benzoic acid (**1-4/8**),[26] 1-hydroxymethyl 15-crown-5 (**2**),[16e] 4′-hydroxymethylbenzo-15-crown-5 (**3**),[16b] methyl 15-crown-5 3,4,5-tris(*n*-dodecan-1-yloxy)benzoate (**4-12/0**, **12-AG-15C5**),[16e] 4′-methylbenzo-15-crown-5 3,4,5-tris(*n*-dodecan-1-yloxy)benzoate (**5-12/0**, **12-AG-B15C5**),[19e] *n*-5,5,6,6,7,7,8,8,9,9,10,10,11,11,12,12,12-heptadecafluorododecyl bromide (**6-4/8**),[26] methyl 3,4,5 tris[*p*-(*n*-dodecan-1-yloxy)-benzyloxy]benzoate (**12-ABG-CH$_3$**),[16b] 3,4,5 tris[*p*-(*n*-dodecan-1-yloxy-)benzyloxy]benzoic acid (**13-12/0**, **12-ABG**),[16c] methyl 15-crown-5 3,4,5-tris[*p*-(*n*-dodecan-1-yloxy)benzyloxy]benzoate (**14-12/0**, **12-ABG-15C5**),[16e] 4′-methylbenzo-15-crown-5 3,4,5 tris[*p*-(*n*-dodecan-1-yloxy)-benzyloxy]benzoate (**15-12/0**, **12-ABG-B15C5**),[16b] and NaOTf[16b] have been reported previously.

**Methyl 15-Crown-5 3,4,5-Tris(*n*-9,9,10,10,11,11,12,12,12-nonafluorododecan-1-yloxy)benzoate (4-8/4, 12F8-AG-15C5).** Compound **4-8/4** was synthesized by the esterification of **1-8/4** and 1-hydroxymethyl-15-crown-5 (**2**) with DCC and catalyzed by DPTS. Compound **1-8/4** (1.20 g, 1.03 mmol), **2** (0.309 g, 1.24 mmol), and DPTS (64 mg, 20 mol %) were dissolved in 10 mL of $CH_2Cl_2$. DCC (0.283 g, 1.37 mmol) was added, and the mixture was heated to reflux. After 12 h, $CH_2Cl_2$ was evaporated on a rotary evaporator. The product was dissolved in hexanes and separated from the insoluble reaction byproducts by filtration. After purification by flash column chromatography [$SiO_2$; $CH_2Cl_2$−$CH_2Cl_2$:MeOH (20:1) gradient], 1.10 g (76.7%) of a clear oil was obtained. Purity (HPLC), 99%; TLC (9:1 $CHCl_3$:MeOH), $R_f$ = 0.2. Thermal transitions and corresponding enthalpy changes are summarized in Table 1. $^1$H NMR ($CDCl_3$, TMS, $\delta$, ppm): 1.37−1.48 (overlapped peaks, 30H, $CF_2CH_2(CH_2)_5$), 1.78 (m, 6H, $CH_2CH_2OAr$), 2.05 (m, 6H, $CF_2CH_2$), 3.68−3.76 (overlapped peaks, 19H, $CO_2CH_2C(H)CH_2(OCH_2CH_2)_4$), 4.01 (overlapped t, 6H, $CH_2OAr$, $J$ = 6.2 Hz), 4.41 (m, 2H, $CO_2CH_2$), 7.26 (s, 2H, *ortho* to $CO_2$); $^{19}$F NMR ($CDCl_3$, $\delta$, ppm): −81.7 (m, 9F, $CF_3$), −115.3 (m, 6F, $CF_2CH_2$), −125.1 (m, 6F, $CF_2CF_2CH_2$), −126.7 (m, 6F, $CF_3CF_2$); $^{13}$C NMR ($CDCl_3$, $\delta$, ppm): 20.0 ($CF_2CH_2CH_2$), 25.9 ($CH_2CH_2CH_2$-OAr), 29.0−29.2 ($CF_2CH_2CH_2CH_2(CH_2)_2$), 30.2 ($CH_2CH_2OAr$), 30.7 ($CF_2CH_2CH_2CH_2$), 31.1 (t, $CF_2CH_2$, $J$ = 22.5 Hz), 64.9 ($CO_2CH_2$), 69.0 ($CH_2OAr$, 3,5-position), 70.4, 70.5, 70.7, 70.9, 71.1 ($C(H)CH_2$-$(OCH_2CH_2)_3OCH_2$, $CH_2C(H)OCH_2$), 73.3 ($CH_2OAr$, 4-position), 77.7 ($CH_2C(H)CH_2$), 108.1 (*ortho* to $CO_2$), 124.8 (*ipso* to $CO_2$), 142.2 (*para* to $CO_2$), 152.7 (*meta* to $CO_2$), 166.1 ($ArCO_2$). Anal. Calcd for $C_{54}H_{71}F_{27}O_{10}$: C, 46.56; H, 5.14. Found: C, 46.71; H, 5.27.

**Methyl 15-Crown-5 3,4,5-Tris(*n*-7,7,8,8,9,9,10,10,11,11,12,12,12-tridecafluorododecan-1-yloxy)benzoate (4-6/6, 12F6-AG-15C5).** From **1-6/6** (1.0 g, 0.73 mmol), **2** (0.19 g, 0.77 mmol), DPTS (42 mg, 0.15 mmol), and DCC (0.20 g, 0.97 mmol) in 5 mL of $CH_2Cl_2$ was obtained 0.70 g (60%) of a clear oil after purification by flash column chromatography (neutral $Al_2O_3$, 2:1 hexanes:ethyl acetate). Purity (HPLC), 99+%; TLC (2:1 hexanes:ethyl acetate), $R_f$ = 0.1. Thermal transitions and corresponding enthalpy changes are summarized in Table 1. $^1$H NMR ($CDCl_3$, TMS, $\delta$, ppm): 1.50 (m, 18H, $CF_2CH_2(CH_2)_3$), 1.84 (m, 6H, $CH_2CH_2OAr$), 2.07 (m, 6H, $CF_2CH_2$), 3.68−3.80 (overlapped peaks, 19H, $CO_2CH_2C(H)CH_2(OCH_2CH_2)_4$), 4.02 (t, 6H,

(40) Gankema, H.; Hempenius, M. A.; Möller, M.; Johansson, G.; Percec, V. *Macromol. Symp.*, in press.
(41) (a) Simon, J.; Sirlin, C. *Pure Appl. Chem.* **1989**, *61*, 1625. (b) Toupance, T.; Ahsen, V.; Simon, J. *J. Chem. Soc., Chem. Commun.* **1994**, 75.
(42) Sielcken, O. E.; van de Kuil, L. A.; Drenth, W.; Schoonman, J.; Nolte, R. J. M. *J. Am. Chem. Soc.* **1990**, *112*, 3086.
(43) (a) Boden, N.; Borner, R. C.; Bushby, R. J.; Clements, J. *J. Am. Chem. Soc.* **1994**, *116*, 10807. (b) Boden, N.; Bushby, R. J.; Clements, J. *J. Chem. Phys.* **1993**, *98*, 5920.
(44) Adam, D.; Schuhmacher, P.; Simmerer, J.; Hänssling, L.; Siemensmeyer, K.; Etzbach, K. H.; Ringsdorf, H.; Haarer, D. *Nature* **1994**, *371*, 141.
(45) (a) Spiess, H. W. *Ber. Bunsenges. Phys. Chem.* **1993**, *97*, 1294. (b) Bengs, H.; Finkelmann, H.; Küpfer, J.; Ringsdorf, H.; Schuhmacher, P. *Makromol. Chem., Rapid Commun.* **1993**, *14*, 445.
(46) Keller, A. *Macromol. Symp.* **1995**, *98*, 1.
(47) de Gennes, P.-G. *Angew. Chem., Int. Ed. Engl.* **1992**, *31*, 842.

C$H_2$OAr, $J$ = 6.2 Hz), 4.41 (m, 2H, $CO_2CH_2$), 7.26 (s, 2H, *ortho* to $CO_2$); $^{19}$F NMR ($CDCl_3$, $\delta$, ppm): −81.4 (m, 9F, $CF_3$, $J$ = 9.6 Hz), −115.1 (m, 6F, $CF_2CH_2$), −122.6 (m, 6F, $CF_2CF_2CH_2$), −123.6 (s, 6F, $CF_3CF_2CF_2CF_2$), −124.2 (s, 6F, $CF_3CF_2CF_2$), −126.8 (m, 6F, $CF_3CF_2$); $^{13}$C NMR ($CDCl_3$, $\delta$, ppm): 20.0 ($CF_2CH_2CH_2$), 25.8 ($CH_2$-$CH_2CH_2OAr$), 28.8 ($CH_2CH_2OAr$, 3,5-position), 28.9 ($CH_2CH_2OAr$, 4-position), 29.0 ($CF_2CH_2CH_2CH_2$, 3,5-position), 30.0 ($CF_2CH_2$-$CH_2CH_2$, 4-position), 30.7 (t, $CF_2CH_2$, $J$ = 22.6 Hz), 64.9 ($ArCO_2CH_2$), 68.8 ($CH_2OAr$, 3,5-position), 70.4, 70.5, 70.7, 70.9, 71.1, 71.2 ($CH_2CH(OCH_2CH_2)_3OCH_2$, $CH_2CH(OCH_2$), 73.1 ($CH_2OAr$, 4-position), 77.7 ($CH_2CH(OCH_2$), 108.1 (*ortho* to $CO_2$), 124.9 (*ipso* to $CO_2$), 142.2 (*para* to $CO_2$), 152.7 (*meta* to $CO_2$), 166.1 ($ArCO_2$). Anal. Calcd for $C_{54}H_{59}F_{39}O_{10}$: C, 40.33; H, 3.70. Found: C, 40.44, H, 3.71.

**Methyl 15-Crown-5 3,4,5-Tris(*n*-5,5,6,6,7,7,8,8,9,9,10,10,11,11,-12,12,12-heptadecafluorododecan-1-yloxy)benzoate (4-4/8, 12F8-AG-15C5).** From **1-4/8** (0.70 g, 0.44 mmol), **2** (0.22 g, 0.88 mmol), DPTS (30 mg, 0.090 mmol), and DCC (0.12 g, 0.58 mmol) in a 50 mL mixture of refluxing $CH_2Cl_2$ and Freon 113 (1:1 ratio) was obtained 0.37 g (46%) of a white, waxy solid after purification by flash column chromatography ($SiO_2$; $CHCl_3$/MeOH gradient, 20:1 $CHCl_3$:MeOH minimum ratio). Purity (GPC), 99+%; TLC (20:1 $CHCl_3$:MeOH), $R_f$ = 0.2. Thermal transitions and corresponding enthalpy changes are summarized in Table 1. $^1$H NMR ($CDCl_3$, TMS, $\delta$, ppm): 1.89 (overlapped peaks, 12H, $CF_2CH_2(CH_2)_2$), 2.14 (m, 6H, $CF_2CH_2$), 3.62−3.82 (overlapped peaks, 19H, $CO_2CH_2C(H)CH_2(OCH_2CH_2)_4$), 4.07 (overlapped t, 6H, $CH_2OAr$), 4.42 (m, 2H, $ArCO_2CH_2$), 7.28 (s, 2H, *ortho* to $CO_2$); $^{19}$F NMR ($CDCl_3$, $\delta$, ppm): −81.4 (m, 9F, $CF_3$, $J$ = 10.0 Hz), −115.1 (m, 6F, $CF_2CH_2$), −122.6 (m, 18F, $(CF_2)_3CF_2CH_2$), −123.4 (s, 6F, $CF_3CF_2CF_2CF_2$), −124.1 (s, 6F, $CF_3CF_2CF_2$), −126.8 (m, 6F, $CF_3CF_2$); $^{13}$C NMR ($CDCl_3$, $\delta$, ppm): 17.1 ($CF_2CH_2CH_2$, 3,5-position), 17.3 ($CF_2CH_2CH_2$, 4-position), 28.7 ($CH_2CH_2OAr$, 3,5-position), 29.7 ($CH_2CH_2OAr$, 4-position), 31.0 (t, $CF_2CH_2$, $J$ = 22.3 Hz), 65.0 ($CO_2CH_2$), 68.4 ($CH_2OAr$, 3,5-position), 70.5, 70.7, 70.9, 71.1, 71.2 ($CH_2C(H)CH_2(OCH_2CH_2)_3OCH_2$, $CH_2C(H)OCH_2$), 72.6 ($CH_2OAr$, 4-position), 77.7 ($CH_2C(H)CH_2$), 108.2 (*ortho* to $CO_2$), 125.3 (*ipso* to $CO_2$), 141.9 (*para* to $CO_2$), 152.5 (*meta* to $CO_2$), 166.0 ($CO_2$). Anal. Calcd for $C_{54}H_{47}F_{51}O_{10}$: C, 35.54; H, 2.60. Found: C, 36.08; H, 2.64.

**4'-Methylbenzo-15-crown-5 3,4,5-Tris(*n*-5,5,6,6,7,7,8,8,9,9,10,10,-11,11,12,12,12-heptadecafluorododecan-1-yloxy)benzoate (5-4/8, 12F8-AG-B15C5).** From **1-12/0** (1.00 g, 0.628 mmol), **3** (0.206 g, 0.691 mmol), DPTS (0.040g, 0.125 mmol), and DCC (0.174 g, 0.835 mmol) in a 50 mL mixture of $CH_2Cl_2$ and Freon 113 (1:1) was obtained 0.80 g (68%) of a white, waxy solid. Purity, (HPLC): 99+%; TLC (20:1 $CHCl_3$:MeOH), $R_f$ = 0.3. Thermal transitions and corresponding enthalpy changes are recorded in Table 1. $^1$H NMR ($CDCl_3$, TMS, $\delta$, ppm): 1.88 (overlapped peaks, 12H, $CF_2CH_2(CH_2)_2$), 2.18 (m, 6H, $CF_2CH_2$), 3.76 (bs, 8H, $(OCH_2CH_2)_2$), 3.94 (m, 4H, $ArOCH_2CH_2O$), 4.05 (overlapped t, 6H, $CH_2OAr$), 4.15 (m, 4H, $ArOCH_2CH_2O$), 5.25 (s, 2H, $CO_2CH_2$), 6.88 (d, 1H, *meta* to $CH_2$, $J$ = 8.0 Hz), 6.96 (overlapped peaks, 2H, *ortho* to $CH_2$); $^{19}$F NMR ($CDCl_3$, $\delta$, ppm): −81.4 (m, 9F, $CF_3$, $J$ = 10.0 Hz), −115.1 (m, 6F, $CF_2CH_2$), −122.6 (s, 18F, $(CF_2)_3CF_2CH_2$), −123.4 (s, 6F, $CF_3CF_2CF_2CF_2$), −124.1 (s, 6F, $CF_3CF_2CF_2$), −126.8 (m, 6F, $CF_3CF_2$); $^{13}$C NMR ($CDCl_3$, $\delta$, ppm): 16.9 ($CF_2CH_2CH_2$, 4-position), 17.1 ($CF_2CH_2CH_2$, 3,5-position), 28.5 ($CH_2CH_2OAr$, 3,5-position), 29.5 ($CH_2CH_2OAr$, 4-position), 30.4 (t, $CF_2CH_2$, $J$ = 22.1 Hz), 66.8 ($CO_2CH_2$), 68.3 ($CH_2OAr$, 3,5-position), 68.3, 68.8, 68.9, 69.3, 70.3, 70.8 (crown ether), 72.5 ($CH_2OAr$, 4-position), 107.9 (*ortho* to $CO_2$), 113.5 (*ortho* to $CH_2$ and O on crown ether), 114.5 (*meta* to $CH_2$ on crown ether), 121.8 (*ortho* to $CH_2$ on crown ether), 125.2 (*ipso* to $CO_2$), 128.8 (*ipso* to $CH_2$ on crown ether), 141.4 (*para* to $CO_2$), 148.8 (*ipso* to O on crown ether), 152.4 (*meta* to $CO_2$), 165.9 ($CO_2$). Anal. Calcd for $C_{58}H_{47}F_{51}O_{10}$: C, 37.20; H, 2.53. Found: C, 37.38; H, 2.49.

**Methyl 4-(*n*-5,5,6,6,7,7,8,8,9,9,10,10,11,11,12,12,12-Heptadecafluorododecan-1-yloxy)benzoate (8-4/8).** Compound **8-4/8** was synthesized by the etherification of **7** with **6-4/8**. Compound **7** (3.56 g, 23.4 mmol) and $K_2CO_3$ (9.69 g, 0.070 mmol) were combined in 130 mL of DMF under a $N_2$ atmosphere. **6-4/8** (13.0 g, 23.4 mmol) was added, and the mixture was heated to 65 °C. After 20 h, the reaction mixture was cooled to room temperature and poured into 1000 mL of ice water. After acidification with dilute HCl, the product was collected by vacuum filtration and dried in air. Recystallization from acetone at 0 °C yielded 12.0 g (81.9%) of white, sheet-like crystals. Purity, (HPLC): 99+%; TLC (2:1 hexanes:ethyl acetate), $R_f$ = 0.7. The following thermal transitions (°C) and their enthalpies of transition (kcal mol$^{-1}$) were observed by DSC (10 °C min$^{-1}$): k 70 (7.83) $s_A$ 81 (1.44) i, on the first heating scan; i 75 (1.48) $s_A$ 52 (5.71) k, on the cooling scan; and k 69 (6.35) $s_A$ 81 (1.45) i, on the second heating scan; $^1$H NMR ($CDCl_3$, TMS, $\delta$, ppm): 1.88 (m, 4H, $CF_2CH_2(CH_2)_2$), 2.17 (m, 2H, $CF_2CH_2$), 3.89 (s, 3H, $CH_3$), 4.06 (t, 3H, $CH_2OAr$, $J$ = 5.5 Hz), 6.89 (d, 2H, *ortho* to O, $J$ = 8.0 Hz), 7.97 (d, 2H, *ortho* to $CO_2$, $J$ = 8.0 Hz); $^{19}$F NMR ($CDCl_3$, $\delta$, ppm): −81.3 (t, 3F, $CF_3$, $J$ = 10.0 Hz), −115.0 (m, 2F, $CF_2CH_2$), −122.4 (m, 6F, $(CF_2)_3CF_2CH_2$), −123.3 (m, 2F, $CF_3CF_2CF_2CF_2$), −124.1 (m, 6F, $CF_3CF_2CF_2$), −126.7 (m, 6F, $CF_3CF_2$); $^{13}$C NMR ($CDCl_3$, $\delta$, ppm): 17.2 ($CF_2CH_2CH_2$), 28.6 ($CH_2$-$CH_2OAr$), 30.6 (t, $CF_2CH_2$, $J$ = 22.0 Hz), 51.8 ($CH_3$), 67.3 ($CH_2OAr$), 114.0 (*ortho* to O), 122.7 (*ipso* to $CO_2$), 162.6 (*ipso* to O), 166.8 ($CO_2$). Anal. Calcd for $C_{20}H_{15}F_{17}O_3$: C, 38.36; H, 2.41. Found: C, 38.46; H, 2.40.

**4-(*n*-5,5,6,6,7,7,8,8,9,9,10,10,11,11,12,12,12-Heptadecafluorododecan-1-yloxy)benzyl Alcohol (9-4/8).** Compound **9-4/8** was prepared by reduction of **8-4/8** with $LiAlH_4$. **8-4/8** (8.0 g, 12 mmol) dissolved in 100 mL of anhydrous $Et_2O$ was added dropwise to a stirred suspension of $LiAlH_4$ (0.52 g, 13 mmol) in 10 mL of anhydrous $Et_2O$. After complete addition, the reaction mixture was stirred for an additional 1.5 h. The reaction was quenched by successive addition of 0.5 mL of $H_2O$, 0.5 mL of 15% NaOH (aqueous), and 1.5 mL of $H_2O$. The granular solids were filtered and rinsed with $Et_2O$. After distillation of $Et_2O$ on a rotary evaporator and recrystallization from acetone at 0 °C, 4.42 g (60.1%) of a white solid was obtained. An additional 1.10 g (15.0%) of pure product was obtained by concentration of the mother liquor and subsequent recrystallization from hexanes: ethyl acetate (1:1). Purity, (HPLC): 99+%. The following thermal transitions (°C) and their enthalpies of transition (kcal mol$^{-1}$) were observed by DSC (10 °C min$^{-1}$): k 92 (6.80) i, on the first heating scan; i 88 (0.20) $s_A$ 81 (6.18) k, on the cooling scan; and k 89, 91 (6.70) i, on the second heating scan; $^1$H NMR ($CDCl_3$, TMS, $\delta$, ppm): 1.86 (m, 4H, $CF_2CH_2(CH_2)_2$), 2.17 (m, 2H, $CF_2CH_2$), 4.01 (t, 2H, $CH_2$-OAr, $J$ = 5.4 Hz), 4.63 (s, 2H, $ArCH_2OH$), 6.91 (d, 2H, *ortho* to O, $J$ = 6.6 Hz), 7.28 (d, 2H, *ortho* to $CH_2$, $J$ = 6.6 Hz); $^{19}$F NMR ($CDCl_3$, $\delta$, ppm): −81.2 (t, 3F, $CF_3$, $J$ = 9.9 Hz), −114.9 (m, 2F, $CF_2CH_2$), −122.4 (m, 6F, $(CF_2)_3CF_2CH_2$), −123.3 (m, 2F, $CF_3CF_2CF_2CF_2$), −124.1 (m, 6F, $CF_3CF_2CF_2$), −126.6 (m, 6F, $CF_3CF_2$); $^{13}$C NMR ($CDCl_3$, $\delta$, ppm): 17.4 ($CF_2CH_2CH_2$), 28.9 ($CH_2CH_2OAr$), 30.8 (t, $CF_2CH_2$, $J$ = 22.0 Hz), 64.9 ($CH_2OH$), 67.3 ($CH_2OAr$), 114.6 (*ortho* to O), 128.8 (*ortho* to $CH_2$), 133.6 (*ipso* to $CH_2$), 158.6 (*ipso* to O). Anal. Calcd for $C_{19}H_{15}F_{17}O_2$: C, 38.14; H, 2.53. Found: C, 38.16; H, 2.46.

**4-(*n*-5,5,6,6,7,7,8,8,9,9,10,10,11,11,12,12,12-Heptadecafluorododecan-1-yloxy)benzyl Chloride (10-4/8).** Compound **10-4/8** was prepared by the chlorination of **9-4/8** with $SOCl_2$. $SOCl_2$ (1.44 g, 12.1 mmol) was added dropwise to a stirring solution of **9-4/8** (5.18 g, 8.67 mmol) in 50 mL of $CH_2Cl_2$ containing a catalytic amount of DMF. After 10 min, the solvent was removed by vacuum distillation. The product was dissolved in $Et_2O$, washed with saturated $NaHCO_3$ and once with water, dried over $MgSO_4$ and filtered. The solvent was removed on a rotary evaporator to yield 5.0 g (94 %) of a white powder which was used in the next step without further purification, mp, 61−62 °C. Purity, (HPLC): 99+%; TLC (4:1 hexanes:ethyl acetate), $R_f$ = 0.8. $^1$H NMR ($CDCl_3$, TMS, $\delta$, ppm): 1.86 (m, 4H, $CF_2CH_2(CH_2)_2$), 2.17 (m, 2H, $CF_2CH_2$), 4.00 (t, 2H, $CH_2OAr$, $J$ = 5.6 Hz), 4.57 (s, 2H, $ArCH_2Cl$), 6.89 (d, 2H, *ortho* to O, $J$ = 8.7 Hz), 7.29 (d, 2H, *ortho* to $CH_2$, $J$ = 8.7 Hz); $^{19}$F NMR ($CDCl_3$, $\delta$, ppm): −81.3 (t, 3F, $CF_3$, $J$ = 9.8 Hz), −115.1 (m, 2F, $CF_2CH_2$), −122.4 (m, 6F, $(CF_2)_3CF_2CH_2$), −123.3 (m, 2F, $CF_3CF_2CF_2CF_2$), −124.1 (m, 6F, $CF_3CF_2CF_2$), −126.7 (m, 6F, $CF_3CF_2$); $^{13}$C NMR ($CDCl_3$, $\delta$, ppm): 17.3 ($CF_2CH_2CH_2$), 28.7 ($CH_2CH_2OAr$), 30.7 (t, $CF_2CH_2$, $J$ = 22.6 Hz), 46.2 ($CH_2Cl$), 67.3 ($CH_2$-OAr), 114.6 (*ortho* to O), 130.1 (*ortho* to $CH_2$), 129.9 (*ipso* to $CH_2$), 159.0 (*ipso* to O).

**Methyl 3,4,5-Tris[*p*-(*n*-5,5,6,6,7,7,8,8,9,9,10,10,11,11,12,12,12-heptadecafluorododecan-1-yloxy)benzyloxy]benzoate (12-4/8, 12F8-ABG-$CH_3$).** Compound **12-4/8** was synthesized according to the same general procedure described for the synthesis of **8-4/8**. From **11** (0.48 g, 2.6 mmol), $K_2CO_3$ (9.7 g, 70 mmol), and **10-4/8** (4.8 g, 7.8 mmol) in 50 mL of DMF was obtained 4.37 g (87.6%) of a white solid after

recrystallization from acetone at 0 °C. Purity, (HPLC): 99+%; TLC (4:1 hexanes:ethyl acetate), $R_f = 0.5$. Thermal transitions and corresponding enthalpy changes are summarized in Table 1. $^1$H NMR ($CDCl_3$, TMS, $\delta$, ppm): 1.87 (overlapped peaks, 12H, $CF_2CH_2(CH_2)_2$), 2.18 (m, 6H, $CF_2CH_2$), 3.89 (s, 3H, $CH_3$), 4.01 (overlapped t, 6H, $CH_2$-OAr), 5.00 (s, 2H, Ar$CH_2$OAr, 4-position), 5.05 (s, 4H, Ar$CH_2$OAr, 3,5-position), 6.76 (d, 2H, *ortho* to O on 4-position, $J = 8.7$ Hz), 6.91 (d, 4H, *ortho* to O on 3,5-position, $J = 8.7$ Hz), 7.27 (d, 2H, *ortho* to $CH_2$ on 4-position, $J = 8.6$ Hz), 7.36 (d, 4H, *ortho* to $CH_2$ on 3,5-position, $J = 8.7$ Hz), 7.37 (s, 2H, *ortho* to $CO_2$); $^{19}$F NMR ($CDCl_3$, $\delta$, ppm): −81.4 (m, 9F, $CF_3$, $J = 9.0$ Hz), −115.0 (m, 6F, $CF_2CH_2$), −122.5 (s, 18F, $(CF_2)_3CF_2CH_2$), −123.4 (s, 6F, $CF_3CF_2CF_2CF_2$), −124.1 (s, 6F, $CF_3CF_2CF_2$), −126.7 (m, 6F, $CF_3CF_2$); $^{13}$C NMR ($CDCl_3$, $\delta$, ppm): 17.3 ($CF_2CH_2CH_2$), 28.7 ($CH_2CH_2OAr$), 30.7 (t, $CF_2CH_2$, $J = 12.5$ Hz), 52.1 ($CO_2CH_3$), 67.2 ($CH_2OAr$, 3,5-position), 71.0 (Ar$CH_2$OAr), 74.7 ($CH_2OAr$, 4-position), 109.2 (*ortho* to $CO_2$), 114.1 (*ortho* to O, 4-position), 114.4 (*ortho* to O, 3,5-position), 124.9 (*ipso* to $CO_2$), 129.0 (*ortho* to $CH_2$, 4-position), 129.3 (*ortho* to $CH_2$, 3,5-position), 129.9 (*ipso* to $CH_2$, 4-position), 130.3 (*ipso* to $CH_2$, 3,5-position), 142.1 (*para* to $CO_2$), 152.7 (*meta* to $CO_2CH_3$), 158.8 (*para* to $CH_2OAr$), 166.5 ($CO_2$). Anal. Calcd for $C_{65}H_{47}F_{51}O_8$: C, 40.56; H, 2.46. Found: C, 40.53; H, 2.41.

**3,4,5-Tris[*p*-(*n*-5,5,6,6,7,7,8,8,9,9,10,10,11,11,12,12,12-heptadecadodecan-1-yloxy)benzyloxy]benzoic Acid (13-4/8, 12F8-ABG).** Compound **13-4/8** was synthesized by the basic hydrolysis of **12-4/8**. Compound **12-4/8** (4.17 g, 2.17 mmol) was dissolved in a refluxing mixture of 50 mL of absolute EtOH and 25 mL of THF. To this solution was added 5 mL of 10 N KOH. After 2 h, the mixture was cooled to room temperature. The mixture was concentrated on a rotary evaporator and redissolved in 500 mL of THF. After acidification with 100 mL of 10% HCl, the mixture was once again concentrated and precipitated into 2 L of ice water. After filtration and recrystallization from acetone, 3.62 g (87.9%) of a white powder was obtained. Purity, (HPLC): 99+%. Thermal transitions and corresponding enthalpy changes are summarized in Table 1. $^1$H NMR ($CDCl_3$/Freon 113, TMS, $\delta$, ppm): 1.89 (overlapped peaks, 12H, $CF_2CH_2(CH_2)_2$), 2.17 (m, 6H, $CF_2CH_2$), 4.03 (overlapped t, 6H, $CH_2OAr$), 5.06 (s, 2H, Ar$CH_2$OAr, 4-position), 5.09 (s, 4H, Ar$CH_2$OAr, 3,5-position), 6.79 (d, 2H, *ortho* to O on 4-position, $J = 8.6$ Hz), 6.93 (d, 4H, *ortho* to O on 3,5-position, $J = 8.7$ Hz), 7.26 (d, 2H, *ortho* to $CH_2$ on 4-position, $J = 8.7$ Hz), 7.38 (d, 4H, *ortho* to $CH_2$ on 3,5-position, $J = 8.7$ Hz), 7.44 (s, 2H, *ortho* to $CO_2$). The $^{19}$F NMR spectrum was not recorded due to the necessity of Freon 113 as a cosolvent. The $^{13}$C NMR spectrum was not recorded due to the low solubility of **13-4/8** in $CDCl_3$/Freon 113 mixtures. Anal. Calcd for $C_{64}H_{45}F_{51}O_8$: C, 40.23; H, 2.37. Found: C, 39.56; H, 2.31.

**Methyl 15-Crown-5 3,4,5-Tris[*p*-(*n*-5,5,6,6,7,7,8,8,9,9,10,10,11,-11,12,12,12-heptadecafluorododecan-1-yloxy)benzyloxy]benzoate (14-4/8, 12F8-ABG-15C5).** Compound **14-4/8** was synthesized according to the same general procedure described for the synthesis of **4-4/8**. From **13-4/8** (1.0 g, 0.53 mmol), **2** (0.15 g, 0.58 mmol), DPTS (0.033 g, 20 mol %), and DCC (0.15 g, 0.71 mmol) in 20 mL of a refluxing mixture of $CH_2Cl_2$:Freon 113 (1:1) was obtained 0.90 g (80%) of a white powder after purification by flash column chromatography [$SiO_2$; $CHCl_3$−$CHCl_3$:MeOH (20:1) gradient). Purity, (HPLC): 99+%; TLC (20:1 $CHCl_3$:MeOH), $R_f = 0.3$. Thermal transitions and corresponding enthalpy changes are summarized in Table 1. $^1$H NMR ($CDCl_3$, TMS, $\delta$, ppm): 1.86 (overlapped peaks, 12H, $CF_2CH_2(CH_2)_2$), 2.17 (m, 6H, $CF_2CH_2$), 3.67−3.84 (m, 19H, $CHCH_2(OCH_2CH_2)_4$), 4.00 (overlapped t, 6H, $CH_2OAr$), 5.00 (s, 2H, Ar$CH_2$OAr, 4-position), 5.04 (s, 4H, Ar$CH_2$OAr, 3,5-position), 6.76 (d, 2H, *ortho* to O on 4-position, $J = 8.5$ Hz), 6.90 (d, 4H, *ortho* to O on 3,5-position, $J = 8.6$ Hz), 7.27 (d, 2H, *ortho* to $CH_2$ on 4-position, $J = 8.5$ Hz), 7.36 (d, 4H, *ortho* to $CH_2$ on 3,5-position, $J = 8.7$ Hz), 7.37 (s, 2H, *ortho* to $CO_2$); $^{19}$F NMR ($CDCl_3$, $\delta$, ppm): −81.4 (m, 9F, $CF_3$, $J = 9.0$ Hz), −115.0 (m, 6F, $CF_2CH_2$), −122.5 (s, 18F, $(CF_2)_3CF_2CH_2$), −123.4 (s, 6F, $CF_3CF_2$-$CF_2CF_2$), −124.1 (s, 6F, $CF_3CF_2CF_2$), −126.7 (m, 6F, $CF_3CF_2$); $^{13}$C NMR ($CDCl_3$, $\delta$, ppm): 17.3 ($CF_2CH_2CH_2$), 28.7 ($CH_2CH_2OAr$), 30.7 (t, $CF_2CH_2$, $J = 12.5$ Hz), 65.0 ($CO_2CH_2$), 67.2 ($CH_2OAr$, 3,5-position), 70.5, 70.6, 70.8, 70.9, 71.0 (crown ether), 71.2 (Ar$CH_2OAr$), 74.7 ($CH_2$-OAr, 4-position), 109.4 (*ortho* to $CO_2$), 114.1 (*ortho* to O, 4-position), 114.5 (*ortho* to O, 3,5-position), 125.1 (*ipso* to $CO_2$), 128.3 (*ortho* to $CH_2$, 4-position), 129.3 (*ortho* to $CH_2$, 3,5-position), 129.9 (*ipso* to $CH_2$, 4-position), 130.3 (*ipso* to $CH_2$, 3,5-position), 142.7 (*para* to $CO_2$), 152.6 (*meta* to $CO_2CH_3$), 158.7 (*para* to $CH_2OAr$), 165.7 ($CO_2$). Anal. Calcd for $C_{75}H_{65}F_{51}O_{13}$: C, 42.03; H, 3.06. Found: C, 42.15; H, 3.03.

**4'-Methylbenzo-15-crown-5 3,4,5-Tris[*p*-(*n*-5,5,6,6,7,7,8,8,9,9,10,-10,11,11,12,12,12-heptadecafluorododecan-1-yloxy)benzyloxy]benzoate (15-4/8, 12F8-ABG-B15C5).** From **13-4/8** (1.0 g, 0.53 mmol), **3** (0.17 g, 0.58 mmol), DPTS (0.033 g, 20 mol %), and DCC (0.15 g, 0.71 mmol) in 20 mL of a refluxing mixture of $CH_2Cl_2$:Freon 113 (1:1) was obtained 0.94 g (81%) of a white powder after recrystallization from acetone. Purity, (HPLC): 99+%; TLC (20:1 $CHCl_3$:MeOH), $R_f = 0.2$. Thermal transitions and corresponding enthalpy changes are summarized in Table 1. $^1$H NMR ($CDCl_3$, TMS, $\delta$, ppm): 1.84 (overlapped peaks, 12H, $CF_2CH_2(CH_2)_2$), 2.17 (m, 6H, $CF_2CH_2$), 3.75 (bs, 8H, $(OCH_2CH_2)_2$), 3.89−4.03 (overlapped peaks, 10H, $CH_2OAr$ and $ArOCH_2CH_2O$), 4.14 (m, 4H, $ArOCH_2CH_2O$), 4.99 (s, 2H, Ar$CH_2$-OAr, 4-position), 5.03 (s, 4H, Ar$CH_2$OAr, 3,5-position), 5.24 (s, 2H, $CO_2CH_2$), 6.76 (d, 2H, *ortho* to O on 4-position, $J = 8.7$ Hz), 6.90 (overlapped peaks, 5H, *ortho* to O on 3,5-position and *ortho* to $CH_2$ on crown ether), 7.26 (d, 2H, *ortho* to $CH_2$ on 4-position, $J = 8.7$ Hz), 7.30 (d, 4H, *ortho* to $CH_2$ on 3,5-position, $J = 8.4$ Hz), 7.37 (s, 2H, *ortho* to $CO_2$); $^{19}$F NMR ($CDCl_3$, $\delta$, ppm): −81.3 (m, 9F, $CF_3$), −115.1 (m, 6F, $CF_2CH_2$), −122.5 (s, 18F, $(CF_2)_3CF_2CH_2$), −123.3 (s, 6F, $CF_3$-$CF_2CF_2CF_2$), −124.1 (s, 6F, $CF_3CF_2CF_2$), −126.7 (m, 6F, $CF_3CF_2$); $^{13}$C NMR ($CDCl_3$, $\delta$, ppm): 17.3 ($CF_2CH_2CH_2$), 28.7 ($CH_2CH_2OAr$), 30.6 (t, $CF_2CH_2$, $J = 12.5$ Hz), 66.8 ($CO_2CH_2$), 67.1 ($CH_2OAr$, 3,5-position), 69.0, 69.1, 69.5, 70.4 (crown ether), 71.0 (Ar$CH_2OAr$), 74.7 ($CH_2OAr$, 4-position), 109.3 (*ortho* to $CO_2$), 113.8 (*ortho* to $CH_2$ and O on crown ether), 114.1 (*ortho* to O, 4-position), 114.4 (*ortho* to O, 3,5-position), 114.7 (*meta* to $CH_2$ on crown ether), 121.9 (*ortho* to $CH_2$ on crown ether), 125.1 (*ipso* to $CO_2$), 128.9 (*ipso* to $CH_2$ on crown ether), 129.1 (*ortho* to $CH_2$, 4-position), 129.5 (*ortho* to $CH_2$, 3,5-position), 129.9 (*ipso* to $CH_2$, 4-position), 130.2 (*ipso* to $CH_2$, 3,5-position), 142.6 (*para* to $CO_2$), 152.6 (*meta* to $CO_2CH_3$), 158.7 (*para* to $CH_2OAr$), 166.1 ($CO_2$). Anal. Calcd for $C_{79}H_{65}F_{51}O_{13}$: C, 43.30; H, 2.99. Found: C, 43.44; H, 2.92.

**Preparation of Complexes of 4-m/n with NaOTf.** Complexes of **4-m/n** with NaOTf were prepared by mixing solutions of **4-m/n** (*ca.* 50 mg/mL) in anhydrous THF with an appropriate volume of a 0.05 M stock solution of NaOTf in THF. The solvent was evaporated under a gentle $N_2$ stream, and the resulting complexes were further dried in a vacuum desiccator over $SiO_2$ under high vacuum for 12−20 h at room temperature.

**Acknowledgment.** Financial support by the National Science Foundation (DMR 92-06781), the Engineering and Physical Research Council, UK and NATO (traveling grant) is gratefully acknowledged. The authors thank Professor S. Z. D. Cheng, University of Akron, for density measurements.

**Supporting Information Available:** DSC traces of semifluorinated blocks or intermediary compounds and of their complexes with NaOTf. Tables of phase transition temperatures and their corresponding enthalpies of transition for all of the complexes of **12Fn-AG-15C5** with NaOTf. Phase diagrams illustrating the dependence of phase transition temperature on the NaOTf/crown ether molar ratio for **12Fn-AG-15C5**. Optical micrographs and bar graphs of building blocks (14 pages). See any current masthead page for ordering and Internet access instructions.

JA9615738